

# The connection of polaritonic chemistry with the physics of a spin glass

Dominik Sidler,<sup>\*,†,‡,¶</sup> Michael Ruggenthaler,<sup>‡,¶</sup> and Angel Rubio<sup>\*,‡,¶,§</sup>

<sup>†</sup>*Laboratory for Materials Simulations, Paul Scherrer Institut, 5232 Villigen PSI, Switzerland*

<sup>‡</sup>*Max Planck Institute for the Structure and Dynamics of Matter and Center for Free-Electron Laser Science, Luruper Chaussee 149, 22761 Hamburg, Germany*

<sup>¶</sup>*The Hamburg Center for Ultrafast Imaging, Luruper Chaussee 149, 22761 Hamburg, Germany*

<sup>§</sup>*Center for Computational Quantum Physics (CCQ) and Initiative for Computational Catalysis (ICC), Flatiron Institute, 162 5th Avenue, New York, NY 10010, USA*

E-mail: dominik.sidler@psi.ch; angel.rubio@mpsd.mpg.de

## Abstract

Polaritonic chemistry has garnered increasing attention in recent years due to pioneering experimental results, which show that site- and bond-selective chemistry at room temperature is achievable through strong collective coupling to field fluctuations in optical cavities. Despite these notable experimental strides, the underlying theoretical mechanisms remain unclear. In this focus review, we highlight a fundamental theoretical link between the seemingly unrelated fields of polaritonic chemistry and spin glasses, exploring its profound implications for the theoretical framework of polaritonic chemistry. Specifically, we present a mapping of the dressed electronic structure problem under collective vibrational strong coupling to the iconic Sherrington-Kirkpatrick

model of spin glasses. This mapping uncovers a collectively induced instability in the dressed electronic structure (spontaneous replica symmetry breaking), which could provide the long-sought seed for significant local chemical modifications in polaritonic chemistry. This mapping paves the way to incorporate, adjust and probe numerous spin glass concepts in polaritonic chemistry, such as frustration, aging dynamics, excess of thermal fluctuations, time-reversal symmetry breaking or stochastic resonances. Ultimately, the mapping also offers fresh insights into the applicability of spin glass theory beyond condensed matter systems and it suggests novel theoretical directions such as *polarization glasses* with explicitly time-dependent order parameter functions.

## 1 Introduction

It is well established that molecular properties and chemical reactions can be influenced by light. Femtochemistry<sup>1,2</sup> and coherent control using ultra-short and high-power lasers attest to this. So on a first glance it may seem straightforward to reach for a similar outcome by using optical cavities instead of laser driving, which has established the emergent field of *polaritonic or QED chemistry* (see Fig. 1).<sup>3-13</sup> There are, however, a few very important differences that make polaritonic chemistry distinct. Firstly, when using lasers one tries to achieve site-selective chemistry usually with coherent, i.e., classical, light fields. In polaritonic chemistry usually a much smaller number of photons couples and their quantum nature becomes important.<sup>3,14</sup> Secondly, in many cases the electromagnetic field inside an optical cavity is zero, i.e., the cavity is not pumped externally, such that only the strong coupling to the quantum and thermal fluctuations lead to modifications.<sup>3,14</sup> Thirdly, and most importantly for this perspective, in most cases the coupling to a single molecule is small, but non-zero even in the thermodynamic limit.<sup>3,15,16</sup> Therefore, only the macroscopic ensemble of molecules *a priori* couples strongly to the photon-field fluctuations. This *collective-coupling regime* leads to a seemingly paradoxical situation: While chemical reactions and the properties of individual molecules are usually considered local in time and space, this traditional

view is challenged in polaritonic chemistry due to strong feedback effects between the microscopic properties and the macroscopic behavior of the ensemble. The unique nature and origin of those feedback effects bridging different scales in time and space will be the main focus of the present review.

Connecting the different scales and isolating the physically relevant mechanism poses a formidable theoretical challenge, which has so far not been resolved satisfactorily due to its complexity (presumably its off-equilibrium glassy nature).<sup>5,17-20</sup> Particularly the origin of why in some molecular ensembles chemical reactions change<sup>21-27</sup> while in others under similar conditions no effect is observed,<sup>28,29</sup> remains elusive. In this article we want to provide a perspective on this conundrum that gives a partial answer and highlights a way forward to understand how the macroscopic behavior of an ensemble of molecules can act back on its individual constituents with the help of the electromagnetic modes of an optical cavity. While, as we will detail in this manuscript, there are many intricacies that need more theoretical and experimental investigations, eventually a relatively simple picture will emerge thanks to the established theoretical concepts of spin glasses. By borrowing ideas from this mature research discipline and applying them to the situation of collective vibrational strong coupling (VSC, i.e., the cavity is resonant to some vibrational degrees of freedom), we will see that the *electronic* polarizations of the individual molecules become synchronized via the cavity. However, since the overall macroscopic polarization of the ensemble is zero, these synchronized polarizations form intricate patterns that are (dynamically) frustrated.<sup>30</sup> That is, if the dynamic polarization of one molecule is flipped (or asynchronous), all the others need to react in a concerted synchronized way. In the following, we will call this situation a *polarization glass*.<sup>20</sup> The underlying electronic frustration effect does not only bridge length but also time scales. It acts back on all the other degrees of freedom such that it provides a necessary seed to trigger stochastic resonances, which together can affect reaction rates (rare events that depend on the details of the thermal ensemble and the local distribution of

the energy in the ensemble) and other molecular properties. Indeed, based on the analogy with the spin glass, one expects non-trivial local and collective off-equilibrium effects even in a global thermal ensemble. Overall, the presented theoretical framework can provide an avenue for numerous future theoretical and experimental developments in the field of QED chemistry.

In the following we will first discuss the theoretical setting for describing VSC in the collective regime (Sec. 2), then show numerical and experimental evidence for frustration and phase-transition-like behavior of a polarization glass (Secs. 3.1-3.2), before we present a novel mapping of the dressed electronic-structure problem onto the prototypical Sherrington-Kirkpatrick (SK) spin glass model (Secs. 3.3-3.4) and introduce corresponding theoretical instability concepts (Secs. 3.5). We will also address theoretical and experimental observables as well as crucial differences between the spin-glass and polarization-glass setups (Sec. 4).

## 2 Pauli-Fierz ab initio theory

As a starting point to describe an ensemble of molecules coupled to an optical cavity one usually employs the Pauli-Fierz theory, which provides a rigorous and non-perturbative theoretical framework to describe the coupling of non-relativistic quantized matter and the quantized light field in an optical cavity (see Fig. 1 for a paradigmatic setup).<sup>8,31</sup> By solving the corresponding Schrödinger-type equation, even strongly coupled light and matter can be accurately described on the atomistic scale. In the case that the enhanced light-modes of the optical cavity have a wavelength much larger than the molecular systems, we can employ the long-wavelength and the few-mode approximation,<sup>8</sup> such that in length-gauge the Pauli-Fierz Hamiltonian takes the form

$$\hat{H} = \hat{H}^m + \frac{1}{2} \left[ \hat{p}_\beta^2 + \omega_\beta^2 \left( \hat{q}_\beta - \frac{\hat{X} + \hat{x}}{\omega_\beta} \right)^2 \right]. \quad (1)$$

For simplicity we have chosen a single-effective cavity mode  $\beta$ , e.g., of a Fabry-Pérot cavity. Notice that more evolved cavity setups can be designed that, e.g., allow for higher mode-volume confinements (such as in plasmonic or micro cavities).<sup>32-36</sup> Moreover, cavity leakage effects of the mirrors are a priori not captured by Eq. (1). However, those could be accounted for by considering multiple modes (broadening) and thus introducing a finite line width (lifetime) based on the imaginary part of the dielectric response of the mirrors.<sup>37,38</sup> The more general minimal-coupling Pauli-Fierz framework is discussed in, for example, Ref. 8, but we do not expect that this more intricate description will qualitatively change the results in the following.

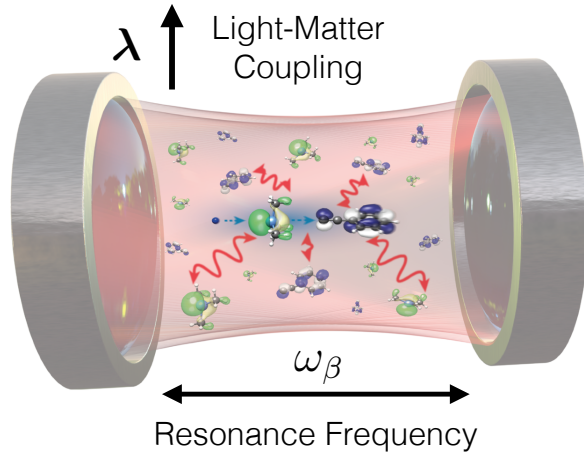


Figure 1: Sketch of a molecular ensemble under vibrational strong coupling (VSC) in a Fabry-Pérot cavity. The distance between the reflective mirrors is inversely proportional the resonance frequency  $\omega_\beta$ , i.e., which photon modes are enhanced due to the standing-wave conditions, and together with the finesse of the mirrors this dictates the single-particle light-matter coupling strength  $\lambda$  (see also Eq. (2)).<sup>5</sup>

In Eq. (1) the free-space matter Hamiltonian is defined as  $\hat{H}^m$ , which accounts for the quantized nuclei and electrons of the molecules. Thus  $\hat{H}^m$  describes the highly non-trivial free-space matter problem, which has been the focus of quantum-chemical methods over many decades. The second term describes the coupling of the matter to the quantized displacement field operator  $\hat{q}_\beta$ , with the conjugate photon operator defined as  $\hat{p}_\beta$ . The matter polarization operators for  $N$  molecules with  $N_n$  nuclei and  $N_e$  electrons are given as

$\hat{X} := \boldsymbol{\lambda} \sum_{i=1}^N \sum_{n=1}^{N_n} Z_n \hat{\mathbf{R}}_{in}$  and  $\hat{x} := -\boldsymbol{\lambda} \sum_{i=1}^N \sum_{n=1}^{N_e} Z_e \hat{\mathbf{r}}_{in}$ , where the nuclear and electronic total transition dipole moments, respectively, are coupled via  $\boldsymbol{\lambda}$  to the effective displacement field mode of frequency  $\omega_\beta$ . The vectorial photon-matter coupling  $\boldsymbol{\lambda} = \boldsymbol{\varepsilon} \lambda$  depends on the mode polarization vector  $\boldsymbol{\varepsilon}$  and the coupling constant<sup>8</sup>

$$\lambda = \sqrt{\frac{e^2}{\mathcal{V} \varepsilon_0}}, \quad (2)$$

where  $\mathcal{V}$  corresponds to the effective mode volume. This effective mode volume can be connected to properties of the Fabry-Pérot cavity and scales roughly as  $L^3 \mathcal{F}$ , where  $\mathcal{F}$  is the finesse of the cavity. A more elaborate discussion reveals that the effective mode volume leads to a finite light-matter coupling even in the macroscopic limit.<sup>16</sup> It is important to highlight two aspects of the Pauli-Fierz theory in the length gauge and the few-mode approximation. Firstly, that we have an equilibrium solution of the coupled system is due to the fact that the light-matter coupling term in Eq. (1) is quadratic and thus the Hamiltonian is bounded from below. Of specific importance for the stability of the coupled system is the term  $(\hat{X} + \hat{x})^2$ , which is quadratic in the coupling strength  $\lambda$ .<sup>39,40</sup> This term is called dipole self-energy or self-polarization term in the literature. Secondly, for the proper free-space continuum limit it is important to subtract the free-space contributions from the effective-mode theory. Otherwise, one would double-count the interaction with the free-space modes that are captured by working with the observable masses of the charged particles.<sup>16</sup> Thus  $\lambda = 0$  means no cavity, and for any Fabry-Pérot cavity there is a finite mode volume  $\mathcal{V}$  which implies  $\lambda > 0$  and also dictates the maximal amount of molecules that can in fact be coherently coupled for a given molecular density. This aspect will become important later when we discuss the scaling behavior in QED chemistry (see Sec. 3.5).

At this point it is important to highlight again that in most experiments in polaritonic chemistry the effective mode volume is large, since many molecules are coherently coupled, and  $\lambda \ll 1$ . Based on this small prefactor it is then often argued that no effect for molec-

ular systems should be observed in a dark cavity. We will, however, not apriori discard the coupling terms. Most importantly because although the prefactor  $\lambda$  might be small, the quadratic coupling term formally scales as  $N^2$  and hence for  $N \gg 1$  this scaling can potentially balance this small prefactor and eventually give rise to a quantitative effect at the single molecular level. Moreover, because in the following we focus on VSC, which implies that the cavity frequency  $\omega_\beta$  is tuned on the vibrational excitations rather than the energetically higher-lying electronic excitations, the cavity Born-Oppenheimer partitioning is a natural and effective choice to proceed.<sup>8,15,41</sup> Thus in a Born-Huang expansion the total wave function is partitioned by grouping the nuclear and displacement field degrees and the electronic wave function is treated as a conditional wave function that depends on the nuclear and displacement coordinates. This allows to write the Hamiltonian for the electronic part of the coupled problem as

$$\hat{H}^e(\mathbf{R}, q_\beta) := H^{\text{m,e}}(\mathbf{R}) + \left( \frac{1}{2} \hat{x}^2 + \hat{x}X - \omega_\beta \hat{x}q_\beta \right), \quad (3)$$

which parametrically depends on all the nuclei positions

$$\mathbf{R} := [\mathbf{R}_1 = (\mathbf{R}_{11}, \dots, \mathbf{R}_{1N_n}), \dots, \mathbf{R}_N = (\mathbf{R}_{N1}, \dots, \mathbf{R}_{NN_n})] \quad (4)$$

and displacement photon field coordinates, written compactly as  $(\mathbf{R}, q_\beta)$ . The free-space electronic-structure problem is given by  $H^{\text{m,e}}(\mathbf{R})$ . Notice that if we would keep all non-adiabatic couplings in the Born-Huang expansion no approximation has been made so far. Only in a next stage, different levels of approximations are introduced to reduce the computational complexity of the fully quantized problem given in Eq. (1), see e.g. Refs. 41,42.

Throughout this work, we are mainly interested in the physical properties of the cavity-mediated electronic structure given in Eq. (3). For this reason, we proceed by applying the classical (for the nuclear and displacement degrees of freedom) cavity Born-Oppenheimer

approximation on the coupled nuclear-photon problem. This allows for a computationally efficient determination of reasonable parameters  $(\mathbf{R}, q_\beta)$  that enter the dressed electronic-structure problem. In more detail, nuclei and (effective<sup>16</sup>) displacement field evolve on the dressed ground-state electronic potential-energy surface according to the classical Hamiltonian dynamics of,<sup>5,20,43–49</sup>

$$H^{\text{npt}} := H^{\text{m,n}}(\mathbf{R}) + \frac{p_\beta^2}{2} + \frac{\omega_\beta^2}{2} \left( q_\beta - \frac{X}{\omega_\beta} \right)^2 + \langle \Psi_0 | \hat{H}^e(\mathbf{R}, q_\beta) | \Psi_0 \rangle. \quad (5)$$

The classical cavity Born-Oppenheimer approximation implies that any quantum and non-adiabatic effects of the nuclear structure are subsequently discarded, which allows for ground-state ab initio molecular dynamic implementations. Such a theoretical setup is numerically feasible even for large molecular ensembles  $N \gg 1$ . We will get back to this adiabatic assumption and discuss its validity in the context of VSC later in Secs. (3.5,4.1,4.2.3). Notice that assuming a classical displacement field  $\mathbf{D} = \lambda \omega_\beta q_\beta / 4\pi$  does not mean that the transverse electric-field operator  $\hat{\mathbf{E}}_\perp$  is entirely classical. Indeed, the transverse electric-field operator is given as,<sup>20</sup>

$$\hat{\mathbf{E}}_\perp = 4\pi(\mathbf{D} - \hat{\mathbf{P}}) \quad (6)$$

within the length-gauge representation used throughout this paper. Thus the electronic part of the macroscopic polarization operator  $\hat{\mathbf{P}} = \lambda(X + \hat{x})/4\pi$  remains fully quantized and describes the electronically bound photons of the hybrid light-matter states.<sup>8,39</sup> The quantized nature of  $\hat{\mathbf{P}}$  will be an essential ingredient for all the subsequent discussions. A further important point is that the displacement field coordinate couples to the *total* dipole of the ensemble and the coupling scales linear in  $\lambda$ . Thus the coupling of the displacement field is different from the direct dipole-dipole coupling due to the self-energy term. Notice further that the longitudinal electric fields remain unaffected by the gauge choice, i.e., they correspond to the standard Coulomb interaction terms of the bare matter problem with classical



nuclei and quantized electrons.

To investigate the physical properties of the dressed electronic problem in Eq. (3), it is convenient to assume the dilute-gas limit for the corresponding many-electron wave function  $\Psi$ , i.e., free-space molecules do not interact with each other described by  $H^{\text{m,e}}(\mathbf{R}) = \sum_{i=1}^N H_i^{\text{m,e}}(\mathbf{R}_i)$ . This is a common choice in the field of polaritonic chemistry, which is applied to a broad range of different situations.<sup>18,20,50–52</sup> We note that this ansatz can also be extended to molecules in more complex environments, such as in solution. In this case  $H_i^{\text{m,e}}(\mathbf{R}_i)$  does not correspond to the electronic structure of a single molecule but to a full solvation shell instead. Assuming non-overlapping electronic structures between the  $N$  molecules, effectively reduces the total electronic wave function  $\Psi$  to a simple Hartree product  $\Psi = \psi_1 \otimes \psi_2 \otimes \cdots \otimes \psi_i \otimes \cdots \otimes \psi_N$  of  $N$  single-molecule electronic wave functions  $\psi_i$ . These single-molecule wave functions are determined by the following  $N$  coupled cavity Hartree (cH) equations,<sup>18,20</sup>

$$\left( H_i^{\text{m,e}}(\mathbf{R}_i) + \left( X - q_\beta \omega_\beta + \sum_{j \neq i}^N \langle \psi_j | \hat{x}_j | \psi_j \rangle \right) \hat{x}_i + \frac{\hat{x}_i^2}{2} \right) \Psi_i = \varepsilon_i \Psi_i. \quad (7)$$

Notice that the mean-field (direct product) description implies no quantum entanglement between the molecules. While in principle one could go beyond a mean-field theory, e.g., using coupled cluster, and other more accurate ab-initio methods<sup>37,53–60</sup> for the collective electronic structure problem, it comes at the cost of increasing the computational load considerably. However, this additional complexity might not be necessary for large molecular ensembles under collective strong coupling, since it has been shown for similar situations that a mean-field treatment becomes exact in the large  $N$ -limit.<sup>61,62</sup> However, the rigorous mathematical analysis of this aspect remains an open research question for the moment. Nevertheless, the subsequently developed connection to a classical spin glass is expected to sufficiently capture the most relevant physical mechanism of the inter-molecularly dressed electronic structure problem under VSC. Certainly, as always, the intra-molecular electronic structure

problem (bare matter) requires the inclusion of exchange and correlation terms to be a chemically accurate description of a molecule. However, this is implicitly enabled by the cH equations. To determine the many-body ground state of the dressed electrons the  $N$  coupled cH equations need to be solved iteratively until convergence. One immediately notices that the recursive dependency on  $\sum_{j \neq i}^N \langle \psi_j | \hat{x}_j | \psi_j \rangle$  may introduce a significant (non-perturbative) modification of the electronic structure, even for small coupling constants  $\lambda$ .<sup>61</sup> This term originates from the quadratic interaction term  $\hat{x}^2$  in Eq. (1) that has the formal scaling of  $N^2$ . Notice, the length gauge representation is convenient to uncover this fundamental all-to-all interaction term. However, it is a gauge independent feature, which is implicitly present in any other gauge (e.g., also in the common velocity gauge).<sup>57,63</sup> It makes the main difference to a free-space ensemble, where for each molecule the instantaneous electronic ground state can be determined independently and the unique electronic many-body ground-state is simple. In the free-space case the macroscopic ensemble has no influence on the individual molecule except of statistically exploring all single-molecule configurations. In the following, we will investigate the consequences of this novel long-range all-to-all interaction, which connects the properties of the macroscopic ensemble to its individual constituents.

### 3 A polarization glass is born

#### 3.1 Collective strong coupling with the cavity Hartree equations

To simulate an ensemble of molecules under VSC one has to propagate the classical equations of motion based on Eq. (5) in contact with a thermal bath.<sup>5</sup> Traditionally such a classical molecular dynamics setup would be considered overall in (canonical) thermal equilibrium.<sup>64</sup> However, things are more intricate in a cavity,<sup>5</sup> i.e., when forming a glassy phase as will be discussed in Sec. 4.2.4. For each propagation time-step the cH Eqs. (7) have to be solved self-consistently for all the electrons. This is numerically very expensive and demanding. Already minimizing the electronic structure problem of a single realistic molecule at a single time-

step in principle poses a formidable challenge.<sup>65</sup> For this reason, a simple anharmonic one-dimensional Shin-Metiu model molecule<sup>66</sup> was used in Ref. 20 that can be solved numerically exactly and captures all relevant aspects to reach a qualitative understanding of an ensemble of molecules under collective VSC. The Shin-Metiu molecule is a paradigmatic and common model to study chemical reactions and conical intersections in- and outside of cavities.<sup>12,67–70</sup> Each Shin-Metiu molecule consists of only one effective electron and nucleus and thus allows a numerically efficient solution of the free-space matter problem. This computationally simple model permitted the efficient exploration of classical cavity-Born-Oppenheimer molecular dynamics at finite temperature up to several 1000 molecules.<sup>20</sup> A first proof that strong collective coupling was reached in these simulations is displayed in Fig. 2, where the dashed blue line shows the collective Rabi splitting of the vibrational mode of the ensemble of Shin-metiu molecules. The two peaks correspond to the collective upper and lower polaritons, hybrid light-matter excitations, from which the field of polaritonic chemistry deduces its name.<sup>3,7,14</sup> The Rabi splitting is asymmetric, since the self-consistent solution captures the change in refractive index due to many molecules inside the optical cavity.<sup>71,72</sup> For a purely harmonic electronic model one can show that this red-shift can directly be related to the static refractive index of the free-space electronic system.<sup>72</sup> Apart from these macroscopic properties, Fig. 2 also shows the averaged hypothetical absorption spectrum of a single molecule in the ensemble (solid blue line). Interestingly we find besides the dark states (vibrational states that decouple from the photon field) that also the local lower polariton is populated. In a next step, the cavity-induced polarization differences

$$\Delta\mu_0 = \langle \hat{\mu}_i \rangle_{0,\lambda=0} - \langle \hat{\mu}_i \rangle_{0,\lambda} \quad (8)$$

were analyzed in the collective electronic groundstate by increasing the number of molecules. However, at the same time the coupling was decreased as  $\lambda/\sqrt{N}$  to see whether the local polarizations persist in the large- $N$  (thermodynamic) limit. The electronic polarization

operator of the  $i$ -th Shin-Metiu molecule is given by  $\hat{\mu}_i = -Z_e \hat{r}_i$ . Indeed, Fig. 3 provides unique microscopic insights on the the scaling statistics of such cavity-induced polarizations. It depicts the first evidence of a cavity-induced local polarization under VSC in the collective-coupling regime.<sup>20</sup> In more detail, the time and ensemble averaged polarizations of the single molecules approach a finite value in the thermodynamic limit (blue). In contrast, the macroscopic polarization (black) quickly drops to a vanishingly small value. Notice, these findings hold qualitatively for an ensemble of aligned as well as randomly oriented molecules.<sup>20</sup> Naturally the question arises why do these small single-molecule polarizations not add up constructively to generate a macroscopic polarization? Here Fig. 3, which shows the time-averaged probability density  $P_{\text{cH}}(\Delta\mu_0)$ , details that overall the ensemble is not polarized, but there is a symmetric polarization ordering, i.e.,

$$E_{\text{cH}}[\Delta\mu_0] = 0 \tag{9}$$

$$\text{Var}_{\text{cH}}[\Delta\mu_0] \neq 0. \tag{10}$$

This already vaguely resembles a spin-glass phase, for which, simply speaking, one observes zero overall magnetization, but ordering of the local spins (magnetization).<sup>73,74</sup>

Furthermore, we notice that the probability density appears relatively rough (almost discontinuous), even though it is an averaged quantity over many vibrational cycles (nuclear time scales). The emergence of such almost discontinuous probability distribution, as well as the very noisy data for the cavity-induced local polarizations (even on a logarithmic scale), suggest the presence of a *frustration* mechanism, i.e., the local polarization patterns are long-lived, despite being constantly perturbed by the vibrating nuclei. Moreover, the frustrated behaviour suggests that the time and ensemble averaged data is strongly correlated with the randomly chosen initial state of the system. This is what one would expect in a spin glass as well.<sup>75</sup> For this reason, the above local polarization pattern with zero net polarization was termed a *polarization glass* in Ref. 20. Eventually, we would like to highlight that

solving the cH equations for the Shin-Metiu molecules numerically is only possible up to a certain collective Rabi-splitting. When increasing the collective coupling strength beyond this value, the self-consistency cycles of the cH equations do not converge anymore.<sup>20</sup> This suggests the emergence of a cavity-induced *phase transition* at a certain collective coupling strength. Again, the occurrence of a phase transition that depends on the strength of an all-to-all interaction term closely resembles the behaviour of a spin glass. In the following we want to further explore the connections of this frustrated polarizations in a cavity and the physics of spin glasses. We expect that this gives us some fundamental microscopic insights into the conundrum of VSC under collective strong coupling. But before, we discuss some experimental evidence for the proposed phase transition.

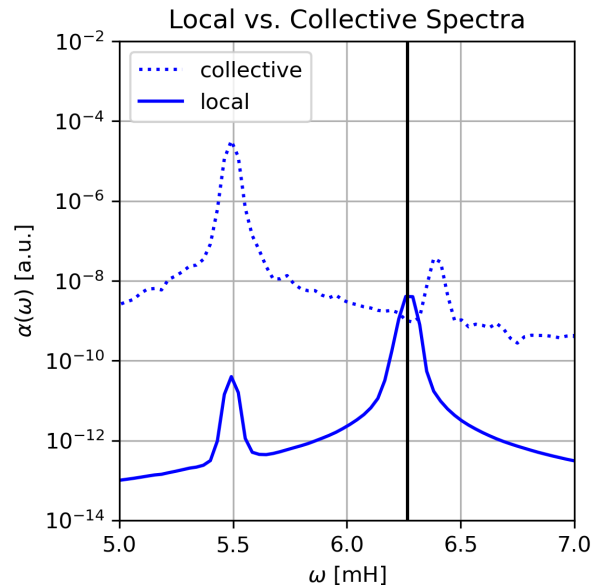


Figure 2: Collective (dotted) vs. local (bold) Rabi splitting for ( $N=900$ ) aligned Shin-Metiu molecules under VSC, taken from Ref. 20. The local upper polariton is hidden in the broadening of the dark states, which occur at the bare cavity frequency (vertical black line). The asymmetry of the collective Rabi splitting with respect to the bare cavity frequency is a consequence of the red-shift that is caused by the polarizability of the medium, i.e., due to the dipole self-interaction term in the Hamiltonian.

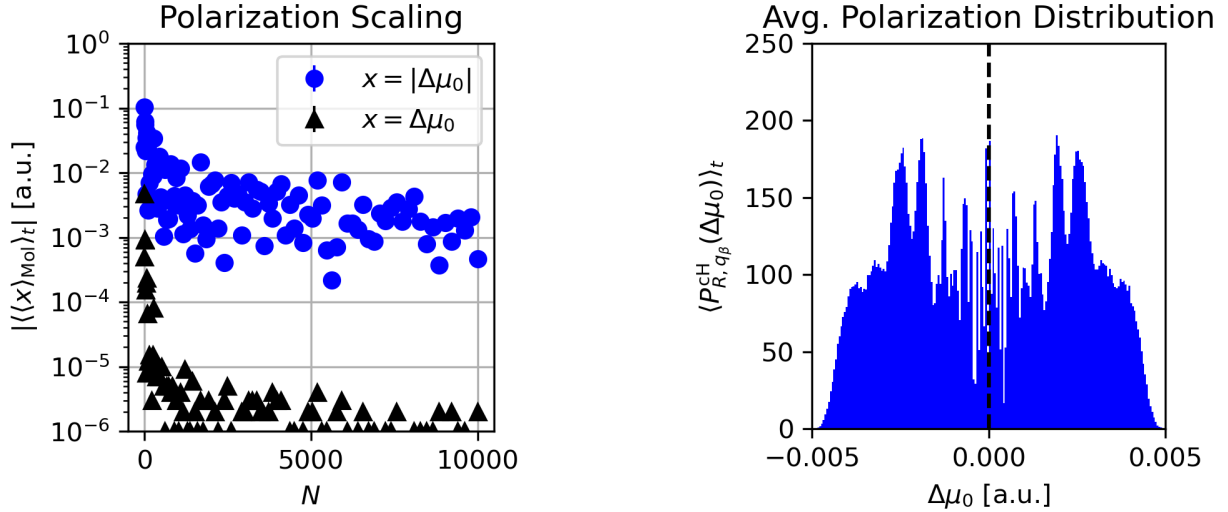


Figure 3: Local polarization features of Shin-Metiu molecules under collective VSC. **Left:** Finite cavity-induced molecular polarizations (blue) that emerge due to the self-consistency cycles of the cH equations (reproduced from Ref. 20). The collective Rabi splitting was kept fixed, when increasing the ensemble size  $N$ . In contrast, the macroscopic polarization (black) quickly drops to zero, within numerical errors. Notice that the numerical results of the Shin-Metiu molecule were determined at the onset of a numerical instability (phase transition), which effectively prevents to reach considerably stronger collective coupling strength with the chosen setup. **Right:** Probability density of the cavity-induced polarizations calculated for  $N = 1024$  molecules of the above setup. The system was equilibrated for 600 time steps and then polarization data was considered from another 600 time steps. Two striking features appear: First, the local polarizations are symmetrically distributed. Second, the probability distribution seems almost discontinuous, even though the electronic-structure data is time-averaged over many vibrational cycles. This should smoothen the data, unless some frustration mechanism counteracts.

### 3.2 Nuclear magnetic resonance experiments

In the previous subsection, we have seen that solving the cH equations reveals several fascinating physical mechanisms in an ensemble of molecules embedded in an optical cavity at ambient temperature  $T$  (polarization ordering, frustration, potential phase transitions). In the following, we compare the above theoretical predictions with recent experimental nuclear magnetic resonance (NMR) results under VSC.<sup>27</sup> In Figs. 4a-c the influence of VSC on the equilibrium concentration between two conformations of a molecular balance sensitive to London dispersion forces is studied with NMR spectroscopy. The experiments reveal that VSC can indeed modify the equilibrium rate constant and thus changes the chemical properties if tuned on resonance with a specific C-H stretching mode of the solute molecules. If we disregard the (important) resonance feature for the moment, the following three experimental observations seem to directly relate to our previous discussions: First, the absence of cavity-induced chemical shifts indicates that the electronic structure is *on average* not polarized by the cavity, which perfectly agrees with what we would anticipate from Eq. (9). Second, the broadening of the chemical shifts seems modified under VSC, which one would expect for a cavity-induced polarization glass, i.e., from Eq. (10). Notice, however, that in Ref. 27 the modified broadening is assigned to experimental artifacts. Nevertheless, it would be interesting to verify if the predicted broadening caused by  $P_{\text{cH}}(\Delta\mu_0)$  contributes to the measured data or if the polarization-glass mechanism is too small to be detected in this NMR setup. The third important insight is an abrupt change of the equilibrium constant at a specific collective strong coupling strength (influenced by the concentration) that does not scale further with the collective Rabi splitting. This suggests a phase transition at a specific collective coupling, as we anticipated from the above discussions about the convergence of the cH equations. Overall, the NMR results of the Ebbesen group seem perfectly in line with the above theoretical description based on the formation of a polarization glass except for one caveat: The observed resonance condition has so far not been studied in detail in the numerical simulations presented above. We will come back to this important aspect at

the end of this review (see Sec. 4.2.3), where we will argue that the resonance mechanism is likely a manifestation of the dynamical aspect of the cavity-induced frustration mechanism.

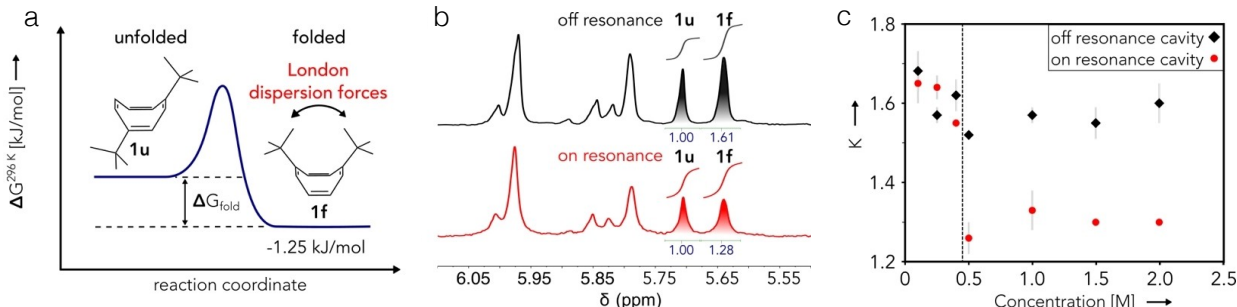


Figure 4: Influence of VSC on the London dispersion-force-driven equilibrium, determined from NMR measurements according to Ref. 27: (a) Free energy difference between folded (1f) and unfolded (1u) conformer in benzened- $d_6$ . (b) On- (red) and off-resonance (black)  $^1\text{H}$  NMR spectra of a 1 M solution. The shaded peaks allow to distinguish the two different conformers. The absence of a frequency shift between the two spectra indicates that on average the electronic structure is not affected (no chemical shift). The magnitude of the peaks can be related to the equilibrium constant between the two conformers, which indicates VSC-induced chemical changes. (c) Varying the concentration (i.e., the collective coupling strength) reveals a critical concentration (dotted line), where suddenly a different conformational equilibrium constant is approached, which suggests the emergence of a cavity-induced phase transition.

### 3.3 Connecting polarization and spin glasses

In the previous sections we have concluded, based on numerical and experimental evidence, that under VSC the cavity-mediated electronic structure seems to form electronic polarization patterns (ordering). Here we want to elucidate these features by comparing to the much better understood physics of spin glasses. That we are using spin glasses as a guideline to understand these polarization effects can be rationalized even pictorially. In Fig. 5 we compare a sketch of a frustrated spin glass with the sketch of a polarization glass. The interaction between the spins/polarizations leads to a frustration effect, where flipping one spin/polarization will force also the others to adapt. We note that usually models of spin glasses are based on (random) short-ranged interactions between spins on a crystal lattice,



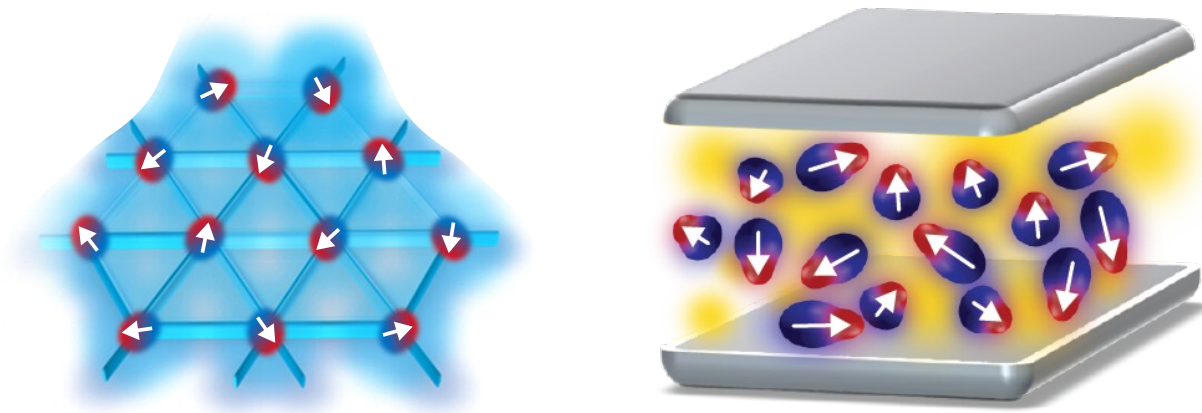


Figure 5: Pictorial comparison of a spin glass and a cavity-mediated polarization glass. **Left:** Spin-frustrated triangular lattice (sketch modified from Ref. 76), whose physical properties can, for example, be modeled by the Edwards-Anderson model,<sup>73</sup> based on (random) short-range interactions between the nearest-neighbour spins on a lattice. **Right:** A dilute molecular polarization glass formed by vibrational strong coupling in optical cavities.<sup>20</sup> Its polarizations can assume continuous values, which are mediated by an all-to-all dipole interactions term instead.

e.g., the Edwards-Anderson model.<sup>73</sup> However, in the polarization-glass case we have a long-range (all-to-all) interaction. While this seems like a very different situation, the best studied spin-glass model, the Sherrington-Kirkpatrick (SK) model,<sup>74,75</sup> is describing almost exactly this case. There are, however, still several distinctions between the case of polaritonic chemistry and standard spin glass systems (models). Most noteworthy is the fact that *a priori* molecular polarizations are continuous. But there are several other distinctions, such as the coupling and back-action to other physical degrees of freedom (displacement and nuclear coordinates), which we will highlight throughout this work and which open up novel research questions at the interface of these two fundamental and distinct research communities.

The Hamiltonian of the SK model of a spin glass is given by

$$H_J(\boldsymbol{\sigma}) = - \sum_{j < i}^N J_{ij} \sigma_i \sigma_j \quad (11)$$

and the couplings  $J_{ij}$  between the spins are independent random variables taken from the

normal distribution  $\mathcal{N}(J_0/N, J^2/N)$ . The presence of an additional external magnetization field  $h$ , acting on the spins as  $\sum_i^N h\sigma_i$  to generate a finite magnetization  $m$ , can be recast into a finite mean-value  $J_0 = h/m$  of the random interactions  $J_{ij}$ .<sup>77</sup> To understand the basic physical properties of the SK model at finite temperature  $T$ , we follow Refs. 75,78 and continue with some definitions. The local ("single molecule") magnetization at temperature  $T$  is given by,

$$m(i)_\alpha = \langle \sigma_i \rangle_{T,\alpha}, \quad (12)$$

where  $\alpha$  denotes a possible quasi-thermal equilibrium state of the SK model, i.e., a local minimum in the phase space for a given choice of  $J$ , at temperature  $T$ . In more detail, the magnetizations  $m(i)_\alpha$  correspond to the  $\alpha$ -th solution of the mean-field equation,<sup>78,79</sup>

$$m(i) = \tanh \left( \frac{\sum_j J_{ij} m(j)}{k_B T} \right), \quad (13)$$

which becomes an exact description for the SK model in the thermodynamic limit.<sup>74,78,80</sup> The determination of the exponentially large number of solutions is a computationally very demanding task. Eventually, the thermal equilibrium ("single molecular") magnetization, averaged over all  $\alpha$  and all possible choices of  $J$ , is defined as

$$m = \langle \langle m(i)_\alpha \rangle_\alpha \rangle_J. \quad (14)$$

We note that averaging over all  $\alpha$  and  $J$  makes the result site-independent, i.e., the left-hand side of Eq. (14) is independent of  $i$ . The numerous fundamental physical properties of the SK model and its implications on polaritonic chemistry will be discussed extensively throughout Secs. 3.5 and 4.

### 3.4 Mapping the cavity Hartree (cH) equations on the Sherrington-Kirkpatrick (SK) model of a spin glass

We have noticed that the continuous all-to-all dipole interaction of the cavity Hartree Eq. (7) resembles the discrete random spin-spin interaction of the SK model in Eq. (11). In the following we show an explicit mapping of the electronic cH equations on the SK model of a spin glass for a specific case. For this purpose and without loss of generality, we look at an ensemble of  $N$  hydrogen-like molecular ions in three dimensions. The single electron free-space Hamiltonian is given in atomic units as<sup>81</sup>

$$\hat{H}_i^m = -\frac{\nabla_{\mathbf{r}_i}^2}{2} - \frac{1}{|\mathbf{r}_{1,i}|} - \frac{1}{|\mathbf{r}_{2,i}|} + \frac{1}{R_i}, \quad (15)$$

with  $\mathbf{r}_{1,i} = \mathbf{r}_i - \frac{\mathbf{R}_i}{2}$  and  $\mathbf{r}_{2,i} = \mathbf{r}_i + \frac{\mathbf{R}_i}{2}$ . Following the common linear combination of atomic-orbital approach of molecular physics, the single-molecule trial wave function is

$$\Psi_i(\mathbf{r}_i) = \frac{a_i\psi(\mathbf{r}_{2,i}) + \sigma_i b_i\psi(\mathbf{r}_{1,i})}{\sqrt{N_i}}, \quad (16)$$

with hydrogen ground-state wave function  $\psi(\mathbf{r}) = e^{-|\mathbf{r}|/a_0}/(\sqrt{\pi}a_0^{3/2})$  at the origin, and normalization  $N_i = \int |\Psi(\mathbf{r}_i)|^2 d\mathbf{r}_i = a_i^2 + b_i^2 + 2\sigma_i a_i b_i I_i$ . Here  $\sigma_i = \pm 1$  will be used to get the simplest possible connection to the classical spins of the SK model. The overlap integral can be evaluated explicitly as:<sup>81</sup>

$$I_i = \langle \psi(\mathbf{r}_{2,i}) | \psi(\mathbf{r}_{1,i}) \rangle = e^{-R_i/a_0} \left( 1 + \frac{R_i}{a_0} + \frac{R_i^2}{3a_0^2} \right) > 0 \quad (17)$$

and the energy of a single molecule eventually becomes,

$$\langle \hat{H}_i^m \rangle = \left( 1 + \frac{(a_i^2 + b_i^2)D_i + 2\sigma_i a_i b_i E_i}{a_i^2 + b_i^2 + 2\sigma_i a_i b_i I_i} - \frac{2a_0}{R_i} \right) E_0 \quad (18)$$

with  $E_0 = -1/(2a_0)$  and analytically evaluated integrals

$$D_i = \langle \psi(\mathbf{r}_{1,i}) | \frac{a_0}{\mathbf{r}_{2,i}} | \psi(\mathbf{r}_{1,i}) \rangle = \frac{a_0}{R_i} \left( 1 - \left( 1 + \frac{R_i}{a_0} \right) e^{-2\frac{R_i}{a_0}} \right) \quad (19)$$

$$E_i = \langle \psi(\mathbf{r}_{1,i}) | \frac{a_0}{\mathbf{r}_{1,i}} | \psi(\mathbf{r}_{2,i}) \rangle = \left( 1 + \frac{R_i}{a_0} \right) e^{-\frac{R_i}{a_0}}. \quad (20)$$

Notice that in contrast to the standard textbook results for  $\text{H}_2^+$ , we have not fixed the pre-factors to  $a_i = b_i = 1$ . This allows for the existence of hydrogen-like molecules with permanent electronic dipole moment (e.g.  $\text{HD}^+$ ) that locally breaks the spatial symmetry of the problem. For a molecular hydrogen ion the  $\sigma_i = 1$  state correspond to a bound state (ground-state), whereas the molecule ionizes/breaks for the state  $\sigma_i = -1$ .<sup>81</sup>

Having represented the free-space problem in terms of the chosen two-level basis in Eq. (16), we can search the collective electronic groundstate that determines the potential-energy surface for the classical nuclear and displacement field dynamics given in Eq. (5). For this purpose, the cH Eqs. (7) are solved until convergence,

$$\min \langle \hat{H}^e \rangle = \sum_i^N \left[ \langle \hat{H}_i^{m,e} \rangle_i - q_\beta \omega_\beta \langle \hat{x}_i \rangle_i + \frac{\langle \hat{x}_i^2 \rangle_i}{2} + 2 \sum_{j < i} \langle \hat{x}_j \rangle_j \langle \hat{x}_i \rangle_i \right], \quad (21)$$

with  $X = 0$  due to the choice of the equally charged nuclear coordinate system. The local integrals can be evaluated explicitly in our two-level basis, assuming the cavity polarization along the molecular axis, i.e., along  $z$  with  $\boldsymbol{\lambda} = \lambda \mathbf{e}_z$ , yielding  $\langle \psi(\mathbf{r}_{1,i}) | \boldsymbol{\lambda} \mathbf{r}_i | \psi(\mathbf{r}_{1,i}) \rangle = -\langle \psi(\mathbf{r}_{2,i}) | \boldsymbol{\lambda} \mathbf{r}_i | \psi(\mathbf{r}_{2,i}) \rangle = \lambda_i R_i / 2$  and  $\langle \psi(\mathbf{r}_{1,i}) | \boldsymbol{\lambda} \mathbf{r}_i | \psi(\mathbf{r}_{2,i}) \rangle = 0$ . The last overlap integral is zero, due to the symmetry of our ground-state hydrogen basis function. Furthermore, we have accounted for the individual orientation of the molecular axis with respect to the cavity polarization by defining  $\lambda_i = \boldsymbol{\lambda} \mathbf{r}_i / |\mathbf{r}_i|$ . Thus we find

$$\langle \hat{x}_i \rangle_i = -\frac{\lambda_i (a_i^2 - b_i^2) R_i}{N_i} \sigma_{i \equiv \pm 1} - \lambda_i (f_i + g_i \sigma_i) \quad (22)$$

with

$$f_i = \frac{(a_i^4 - b_i^4)R_i}{(a_i^2 + b_i^2)^2 - 4a_i^2b_i^2I_i^2} \quad (23)$$

$$g_i = -\frac{2a_ib_iI_i(a_i^2 - b_i^2)R_i}{(a_i^2 + b_i^2)^2 - 4a_i^2b_i^2I_i^2}. \quad (24)$$

Notice,  $\langle \hat{x}_i \rangle_i = 0$  for perfectly symmetric wave functions (i.e. for  $a_i^2 = b_i^2 = 1$ ). For the chosen minimal two-level approximation, the molecule must possess a permanent electric dipole-moment, i.e.,  $a_i^2 \neq b_i^2$ , such that the all-to-all interaction can be captured. Otherwise, our minimal model is too simplified such that it will not show any dependence on the main term we want to investigate. Therefore, we continue by assuming a dimer molecule (e.g. HD<sup>+</sup>) with a permanent electric dipole moment. Furthermore, we discard the purely local term  $\frac{\langle \hat{x}_i^2 \rangle_i}{2}$  for simplicity, since in the large- $N$  limit it will become negligible in our restricted basis set. Therefore, using Eqs. (21) and (22), discarding the constant energy contributions (which naturally excludes  $\sigma_i^2 = 1$  as well) leaves us with the following minimization problem

$$\min_{\sigma} \langle \hat{H}^e \rangle \sim \min_{\sigma} \sum_i [h_{m,i} + \lambda_i(h_{q,i} - h_{d,i})] \sigma_i + 2 \sum_{j < i} \lambda_i \lambda_j g_j g_i \sigma_i \sigma_j. \quad (25)$$

Here external magnetization field-like parameters have been subsumed in a bare-matter term  $h_{m,i}$ , a displacement-field term  $h_{q,i} = q_{\beta} \omega_{\beta} g_i$  and eventually  $h_{d,i} = 2g_i \sum_j^N \lambda_j f_j$  arises from the dipole self-energy. The resulting energy minimization problem in Eq. (25) already resembles the SK model of Eq. (11) at zero temperature, but with an externally applied magnetization field that is  $i$ -dependent instead of a constant. A subtle but important difference here is that for the polarization glass, the "external magnetization field" will depend itself on the solution of the electronic problem in a complete ab-initio molecular dynamics setup. In other words, the electronic system is itself only a subsystem that is correlated with the other (nuclear and displacement) subsystems. We will discuss the impact of this important difference on the description of polaritonic chemistry in Sec. 4. Here, in order to

connect our polaritonic energy minimization model for the instantaneous electronic many-body wave function to established results, we additionally impose the following two physical assumptions:

First, we assume that the molecules are randomly oriented in the molecular ensemble and therefore  $h_{d,i} \propto \sum_j^N \lambda_j f_j \rightarrow 0$ . Thus in Eq. (25) the double sum  $\sum_i^N 2g_i \sigma_i (\sum_j^N \lambda_j f_j) \rightarrow 0$ , while for the single sum we have  $\sum_i^N \lambda_i h_{q,i} \sigma_i \neq 0$  in general. Second, we assume that the temperature of the molecular ensemble is sufficiently low, such that all molecules cannot only be considered in their electronic, but also in their vibrational ground-state and thus  $R_i \rightarrow R$ , which implies  $f_i \rightarrow f$ ,  $g_i \rightarrow g$  and  $h_{m,i} \rightarrow h_m$ . Later we will relax this assumption, after having introduced necessary theoretical tools to capture corresponding thermal effects. Moreover, since the system is in the vibrational and electronic ground state, it is reasonable to impose the zero-transverse-field condition<sup>5</sup>  $\langle \hat{E}_\perp \rangle = 0$ . This leads in our model to  $\sum_i \lambda_i h_{q,i} \sigma_i = -\omega_\beta^2 q_\beta^2$ , which is a constant energy offset that can be discarded in the energy minimization. By the static zero-field condition we have effectively removed the dependence on the displacement-field subsystem, since it is then completely determined by the nuclear and electronic configuration. This also removes the dynamical aspects of the cavity, and hence the mapping can only capture the static aspects of the polaritonic problem under VSC. Dynamical aspects such as the resonance condition will be discussed later in Sec. 4.2.4. With these assumptions/simplifications we find

$$\min_{\sigma} \langle H^e \rangle \sim \min_{\sigma} \sum_i h_m \sigma_i + 2 \sum_{j < i} \lambda_i \lambda_j g^2 \sigma_i \sigma_j. \quad (26)$$

The energy-minimization problem in Eq. (26) corresponds exactly to the SK model at zero temperature if we assume a normal random distribution, i.e., by setting  $2\lambda_i \lambda_j = -J_{ij}$ , where the external magnetization field-like term is absorbed by the mean  $J_0 = h/m$  of the randomly distributed numbers  $J_{ij}$ .<sup>77</sup> The emergence of a cavity-induced polarization structure can then be directly deduced from the magnetization of the SK model. That is, in analogy one looks

at the electric dipole moment operator  $\hat{\mu}_i := R_{i1} + R_{i2} - \hat{r}_i = -\hat{r}_i$  along the symmetry axis of a single HD+ molecule,

$$\hat{\mu}_i = -(f + g\sigma_i), \quad (27)$$

where we used Eqs. (15) and (22) with  $f_i, g_i \mapsto f, g$ . In more detail, any deviation from the uncoupled thermal equilibrium polarization can be interpreted as a *cavity-induced molecular polarization phenomenon*

$$\Delta\mu_T = \langle \hat{\mu}_i \rangle_{T,\alpha,\lambda=0} - \langle \hat{\mu}_i \rangle_{T,\alpha,J}. \quad (28)$$

The brackets denote thermal,  $\alpha$  and  $J$ -averaging, where the later corresponds to the averaging over all possibly realizations of randomly drawn  $J_{ij}$  interactions. Similar to the magnetization of the SK model in Eq. (14), the left-hand side becomes independent of  $i$ . At zero temperature (and thus in the electronic groundstate), a seemingly simple expression is found for the cavity-induced polarization

$$\Delta\mu_0 = |g|(1 - m), \quad (29)$$

where the equilibrium "magnetization"  $m$  must be determined by averaging over the highly-degenerate molecular electronic ground state. That is, if we take the definition of Eq. (12) but use the "spin" quantity  $\sigma_i$  from the polaritonic model of Eq. (16), we find an average "magnetization" of the molecules from Eq. (14). Notice, however, the total polarization of the molecular ensemble will still be zero, since the molecules are randomly oriented within the molecular ensemble, which averages out any local polarization effects. Its unique features will be explored in the following, with possible implications on the mechanistic understanding of VSC and polaritonic chemistry/materials in general. Our subsequent theoretical considerations are guided by Giorgio Parisi's works in particular his Nobel lecture.<sup>75</sup>

### 3.5 The static instability of the Sherrington-Kirkpatrick model

Before we continue characterizing the different phases of the SK model, we introduce the Edwards-Anderson order parameter or self-overlap<sup>73</sup>

$$q_{EA} = \frac{\sum_i m(i)_\alpha m(i)_\alpha}{N} = \text{const. } \forall \alpha, J, \quad (30)$$

which can be shown to neither depend on the state  $\alpha$  nor the specific realization of  $J$ .<sup>75,78</sup> Based on the magnetization  $m$  and the magnetic order parameter  $q_{EA}$ , Sherrington and Kirkpatrick determined an analytical phase diagram in the thermodynamic limit  $N \rightarrow \infty$ . Their computations suggested the emergence of three different phases: a ferromagnetic ( $q_{EA} \neq 0$ ,  $m \neq 0$ ), a spin glass ( $q_{EA} \neq 0$ ,  $m = 0$ ) and a paramagnetic one ( $q_{EA} = 0$ ,  $m = 0$ ). However, Sherrington and Kirkpatrick already noticed that their solution seemed questionable at low temperatures, since it gave rise to a negative entropy, which is nonphysical.<sup>74</sup> Indeed, Almeida and Thouless showed that the original solution of the SK model becomes unstable in the thermodynamic limit at sufficiently low temperature, which leads to the corrected phase diagram of the SK model displayed in Fig. 6.<sup>77</sup> Almeida and Thouless could determine an explicit stability criterion at low temperature for the SK model<sup>77</sup>

$$k_B T > \frac{4}{3\sqrt{2\pi}} J e^{-\frac{J_0^2}{2J^2}}. \quad (31)$$

The striking feature of this result is that in the ground state ( $T \rightarrow 0$ ), the solution of the SK model becomes unstable, and thus enters the spin-glass phase, even if  $\infty > J_0 \gg J$ , i.e., even if the system is exposed to very strong external magnetization fields. This has important implications on our adiabatic polaritonic ground-state minimization problem at zero temperature given in Eq. (26). For this problem  $J_0$  corresponds to the local free-space electronic structure problem. Therefore, we expect that for sufficiently large  $N$  in the molecular ensemble we enter the polarization-glass phase for the dressed electronic ground



state, even for a Hamiltonian dominated by the free-space electronic structure  $J_0$ . That is, even for an arbitrarily small (!) coupling to a cavity  $J \propto \lambda^2 > 0$  there will be an instability at sufficiently large ensembles (see Fig. 6). The SK analogy also indicates that the (electronic) temperature may no longer be discarded when treating the dressed electronic structure under VSC. Consequently, the adiabatic assumption of the cH molecular dynamics can also break down (see discussions in Sec. 4.1). The origin of the Almeida and Thouless instability can be attributed to spontaneous replica symmetry breaking, introduced by an all-to-all interaction term.<sup>75</sup> Notice further, that a spin glass is conceptually distinct from the Anderson localization mechanism, which have been discussed in the context of polaritonic transport properties.<sup>82,83</sup> The fundamental concept of replica symmetry breaking together with its many physical implications will be discussed later in Sec. 4.<sup>77</sup>

At this point an important remark has to be made. So far we have not mentioned any scaling properties of the light-matter coupling parameter  $\lambda$  with respect to the number of molecules  $N$ . In polaritonic chemistry it is usually argued based on the Tavis-Cummings model that the collective coupling strength (i.e., the Rabi splitting) increases with  $\sqrt{N}$ , where  $N$  corresponds to the number of non-overlapping two-level emitters that are collectively coupled. Based on this considerations one would expect that the cavity-mediated dipole-dipole interaction (polarization) between two molecules scales as  $\lambda^2 \propto J_{ij} \propto 1/N$ . However, the analytic SK model imposes  $\lambda^2 \propto J_{ij} \propto 1/\sqrt{N}$  to allow for a spin glass instability (phase) at finite temperatures  $T > 0$  in the thermodynamic limit. Notice, however, at zero temperature the instability persists in any case for  $\lambda > 0$ . Nevertheless, things are more delicate for the cH equations, since the detailed scaling behavior of a macroscopic ensemble of molecules remains largely unexplored. As is highlighted in the discussion after Eq. 2, there is only a finite albeit very large number of molecules coherently coupled and hence the extrapolation to  $N \rightarrow \infty$  becomes intricate. Yet, the numerical results suggest that a non-trivial result appears provided enough molecules couple (see Fig. 3).

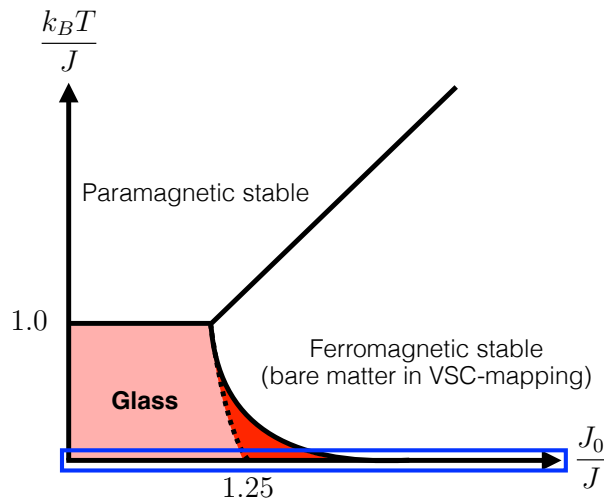


Figure 6: Phase diagram of the SK model, reproduced from Ref. 77 and adjusted for the polaritonic interpretation. The dotted line corresponds to the original (erroneous) spin / polarization glass phase of Sherrington and Kirkpatrick, which did not consider that spontaneous replica symmetry breaking can occur. Replica symmetry breaking extends the (unstable) spin glass regime at low temperature to much larger  $J_0/J \gg 0$  values (dark red). Notably, in the groundstate ( $T \rightarrow 0$ ), the instability occurs for arbitrarily large (but finite)  $J_0$ -values, provided that  $J > 0$  (blue regime).

## 4 Perspective: What can we anticipate from spin-glass theory for polaritonic systems?

In the previous sections we have established a formal connection between the physics of spin glasses and the electronic structure of a molecular ensemble under VSC. Thanks to the theoretical similarities between both problems, we are confident that the polaritonic-chemistry community can learn from established knowledge of the spin-glass community. In particular the understanding of how global fluctuations can lead to significant local modifications of molecular ensembles that can influence how chemical reactions proceed locally. To use this connection seems natural for multiple reasons: First, the SK model provides a paradigmatic model of a spin glass, for which exact results have been determined after decades of intensive research that ultimately were awarded with the Nobel prize in physics (2021).<sup>75</sup> Second, despite the seemingly simple nature of the SK model, it has proven to capture and predict

different complex physical mechanisms that have been confirmed for real materials. Third, the study of the SK model provides novel mathematical ideas to describe and understand those unique physical mechanisms precisely and present the essentials in a compact form. Fourth, the general features of the SK model are quite robust, since it serves as a limiting case<sup>78</sup> for the Bethe lattice model,<sup>84</sup> the long-range Edwards-Anderson model and the infinite dimensional Edwards-Anderson model.<sup>73</sup> In addition, spin-glass models have proven to predict certain features of much more complex structural glasses as well.<sup>78</sup>

## 4.1 Free energy and spontaneous replica symmetry breaking

In order to better understand the origin and physical consequences of the SK model defined in Eq. (11), we have a closer look at the average free energy  $F$ , which can be defined as follows in the thermodynamic limit  $N \rightarrow \infty$ ,<sup>75</sup>

$$F(T) = - \lim_{N \rightarrow \infty} \frac{\overline{k_B T \log(Z_J(T, N))}}{N} \quad (32)$$

$$Z_J(T, N) = 2^{-N} \sum_{\{\sigma\}} e^{-H_J(\sigma)}. \quad (33)$$

The overline indicates the averaging of the partition function  $Z_J$  with respect to randomly drawn  $J_{ij}$  realizations. To simplify the  $J$ -averaging, the so-called replica trick was proposed, where instead of one system with  $N$ -spins, an extended system consisting of  $n$ -times the same system made of  $N$ -spins is considered. It simplifies taking the logarithm as follows<sup>75</sup>

$$F_n(T) = - \lim_{N \rightarrow \infty} \frac{\overline{k_B T (Z_J(T, N))^n}}{nN} \quad (34)$$

$$F(T) = \lim_{n \rightarrow 0} F_n(T) \quad (35)$$

The replica trick works if the  $F_n$  is analytic in  $n$  and has no singularities.<sup>75</sup> In particular, one would expect replica symmetry to hold as a natural assumption, since it implies the re-shuffling of the  $n$  identical replicas will not change the result. From this symmetry aspect,

one can deduce that the free energy depends on a single order parameter  $q$ , which then can be minimized to determine the alleged solution of the SK model.<sup>74,75</sup> However, it turns out that  $F_n$  is indeed not analytic for  $n < n_c < 1$  in the SK model. This indicates that the replica symmetry is spontaneously broken and thus things become much more complex. After a long endeavour the exact solution of the replica Ansatz was discovered by Parisi yielding the following free energy<sup>80,85</sup>

$$F = \max_{\mathcal{q}(x)} F[\mathcal{q}(x)] \quad (36)$$

where the corresponding partial differential equations are given explicitly in footnote <sup>a</sup>. Considerably later it was also proven that the exact solution of the replica ansatz indeed determines the exact free energy of the original problem.<sup>86,87</sup> For the subsequent discussions this solution will be of minor relevance. However, the emergence of an order function  $\mathcal{q}(x)$ , instead of just an order parameter  $q$ , will be essential for the mechanistic understanding of spin glasses in general.

In more detail, explicit expressions were found that relate the order parameter function  $\mathcal{q}(x)$  to the probability density

$$P_J(\mathcal{q}) = \sum_{\alpha\gamma} w_\alpha w_\gamma \delta(\mathcal{Q}_{\alpha\gamma} - \mathcal{q}), \quad (37)$$

of finding two states with overlap

$$\mathcal{Q}_{\alpha\gamma} = \frac{\sum_i m(i)_\alpha m(i)_\gamma}{N} \quad (38)$$

---

<sup>a</sup>

$$\begin{aligned} F[\mathcal{q}(x)] &= -\frac{1}{4k_B T} \left[ 1 + \int_0^1 dx \mathcal{q}^2(x) - 2\mathcal{q}(1) \right] - k_B T f(0, 0) \\ \frac{\partial f(x, h)}{\partial x} &= -\frac{1}{2} \left[ \frac{\partial^2 f}{\partial h^2} + x \left( \frac{\partial f}{\partial h} \right)^2 \right], \end{aligned}$$

with  $f(1, h) = \ln(2 \cosh(h/k_B T))$ .

in a given sample  $J$ . The statistical weights of solution  $\alpha$  are indicated by  $w_\alpha$ .<sup>78</sup> Notice the connection of  $\mathcal{Q}_{\alpha\gamma}$  to the Edwards-Anderson order parameter or self-overlap  $\mathcal{Q}_{\alpha\alpha} = q_{EA}$ . An astonishing feature of spin glasses in general is that  $P_J(\boldsymbol{q})$  shows a dramatic dependency on the specific choice of  $J$  even in the thermodynamic limit (see e.g., left of Fig. 7 for the Edwards-Anderson model without external magnetization fields). A smooth curve is only achieved by averaging over all possible realizations  $J$  (see Fig. 10a) yielding the equilibrium overlap

$$P(\boldsymbol{q}) = \overline{P_J(\boldsymbol{q})}. \quad (39)$$

Eventually, the functional dependency of  $\boldsymbol{q}(x)$  can be made explicit by inverting the probability density

$$x(\boldsymbol{q}) = \int_0^{\boldsymbol{q}} d\boldsymbol{q}' P(\boldsymbol{q}'). \quad (40)$$

Notice, a signature of replica symmetry breaking<sup>75</sup> is the deviation of  $P(\boldsymbol{q})$  from two delta functions at  $\boldsymbol{q} = \pm q_{EA}$  as illustrated in Fig. 10a.

In a next step, we apply the concept of an order parameter distribution on the numerically solved cH equations, aiming to better understand the similarities between molecular polarization and spin glasses. Looking at the probability distribution of the cavity-induced polarization  $P_{R,q_\beta}^{\text{cH}}(\Delta\mu_0)$ , we find a discrete pattern when solving the cH equations for two different parameter choices  $R, q_\beta$  (see Fig. 7). To interpret the similarities as well as differences between the two distributions, we need to have a closer look at the imposed physical conditions for solving the cH equations numerically. As described in Sec. 3.1, the cH equations can only be converged for moderate collective-coupling situations. This suggests that the unique free-space electronic ground state is modified by the cavity, but it is still non-degenerate for a given parameter choice  $R, q_\beta$  and thus the adiabatic assumption still holds. Therefore, when applying the definition of Eq. (37) for the cH setup with  $m(i)_{\alpha_0} \mapsto \Delta\mu(i)_{0,R,q_\beta}$ , one

finds for the cH equations at the onset (!) of the instability ,

$$P_{R,q\beta}^{\text{cH}}(q) = \sum_{\alpha\gamma} w_\alpha w_\gamma \delta(\mathcal{Q}_{\alpha\gamma} - q) = \delta(\mathcal{Q}_{\alpha_0\alpha_0} - q) \quad (41)$$

$$\Rightarrow q = q_{EA}(R, q_\beta) = \sum_i^N \frac{\Delta\mu(i)_{0,R,q\beta}^2}{N}. \quad (42)$$

The unique non-zero weight  $w_{\alpha_0} = 1$  applies within the adiabatic regime of a unique collective ground state, as indicated by  $\alpha_0$ . In contrast to the Edwards-Anderson order parameter of the SK model, we find now a clear parametric dependency on  $q_{EA}(R, q_\beta)$  when applying Eq. (42) on the two numerical distributions in Fig. 3. Hence, the cH equations introduce an order-parameter distribution (see Fig. 3) when averaged over many realizations of  $q_{EA}(R, q_\beta)$  even if only one solution of the cH equations has non-zero weight. Thus the necessity of having the replica symmetry broken is relaxed in contrast to the SK model.

A further important difference between the idealized SK model and the cH equations concerns the different time-scales introduced by the other subsystems, when part of the ab-initio molecular dynamics setup. In the SK model a chosen realization of  $J$  is considered to persist for a very long time-scale, which allows the (thermal) exploration of different (frustrated) local minima  $\alpha$ . In contrast,  $q_{EA}(R, q_\beta)$  oscillate non-perturbatively on a rotational, vibrational and displacement-field time-scale, which is not present in the static picture of the SK mean-field Eq. (13). Notice that despite this non-perturbative local impact, electronic frustration (correlation) effects persist for the cH equations even on those vastly different time-scales (see the discussion in Sec. 4.2.2).

Despite these differences: What can we anticipate from the SK model that is relevant to our understanding of polaritonic chemistry? To better understand the applicability of the SK model, let us now further increase the collective strong coupling of the cH equations such that their ground-state becomes degenerate. Therefore, one can no longer impose the initial adiabatic assumption. This has two immediate consequences: First, similar to the SK model, thermal effects must be included when solving the dressed electronic problem,

even-though the thermal energy scale can be orders of magnitude smaller than the free-space excitation of the electronic structure of a single molecule. This can be rationalized by the fact that the novel collective electronic excitations can be on a much lower energy scale similar to solid-state systems. Second, the resulting non-adiabatic quantum dynamics of the dressed electrons may be seen as an exploration of the different energetic minima for a fixed  $q_{EA}(R, q_\beta)$  parameter choice. This implies that the Dirac-like distribution of  $F_{R, q_\beta}^{\text{cH}}(\Delta\mu_0)$  will be broadened/modified and thus should approach the familiar distribution of spin glasses (possibly re-introducing replica symmetry breaking for the cH equations). Putting it differently, we can now interpret the SK model as the limiting case of infinitely slow dynamics  $(R, q_\beta)$  (quasi-static picture) assuming a constant Edwards-Anderson order parameter  $q_{EA}(R, q_\beta) = q_{EA}$ . Whether the latter assumption is justified in the large- $N$  limit of the cH equations remains an open question. Nevertheless, the quasi-static picture of the SK model should provide physical insight when the adiabatic picture breaks down at sufficiently strong collective couplings. In the following, we will further explore properties of the SK model in the context of polaritonic chemistry. However, we already note at this point that the quasi-static picture will not provide access to cavity-induced resonance effects, which do require feedback effects on a vibrational time-scale. We will discuss this aspect later in Sec. 4.2.4 .

## 4.2 Probing the existence of a polarization glass phase

From the previous discussion it seems possible that VSC in optical cavities can trigger a polarization glass phase for a large number of molecules in the ensemble. While early experimental evidence is in line with this theoretical idea (see Sec. 3.2), it is far from being a confirmation. In the following, we propose specific experimental observables that are promising candidates to investigate and demonstrate the existence of the proposed polarization-glass phase. For this purpose, we re-interpret unique experimental features of spin-glass experiments in the context of the SK model and link them to our polaritonic setup. From an experimental point

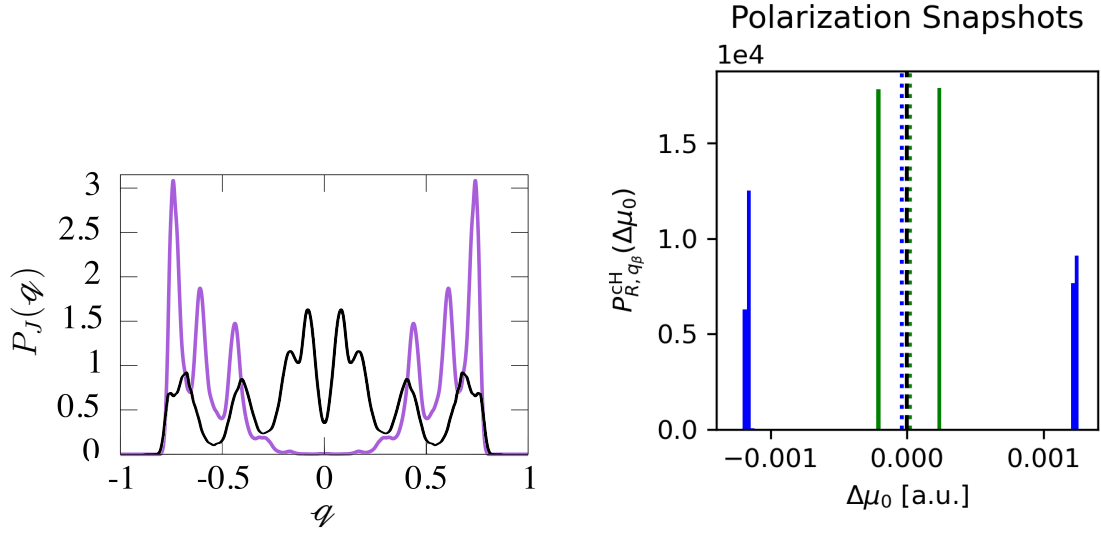


Figure 7: Comparison of the order parameter distribution of a spin glass and the polarization distribution in a polarization glass. **Left:** Example of two rough probability distributions  $P_J(q)$  of the overlap  $q$  for an Edwards-Anderson model of a spin glass without external magnetic field (aggregated from Ref. 75 based on data from Refs. 88,89). The different realizations of  $J$  show large deviations even in the thermodynamic limit. **Right:** Likewise, two (discretely) distinguishable polarization distributions are arising by individually converging the cH equations for two different realizations of parameter sets  $(R, q_\beta = 0)$  (Shin-Metiu setup with  $N = 1024$  molecules).



of view, a characterization of a spin glass is usually done by varying the temperature and applying external magnetization field perturbations  $h'$  as

$$H'_J(\boldsymbol{\sigma}) = h' \sum_i \sigma_i. \quad (43)$$

In our polaritonic picture, this is equivalent to changing the (dressed electronic) temperature or applying a small external electric field perturbation.

#### 4.2.1 Equilibrium Susceptibilities

The hallmark of replica symmetry breaking in spin glass theory can be attributed to the emergence of two different static equilibrium susceptibilities,<sup>78</sup> which are observed in experiments<sup>90</sup> and in the SK model.<sup>30</sup> The two extreme cases describe the response of the system subject to a small external field perturbation. In the so-called zero-field cooled case, the system remains inside a given state while changing the magnetization (electric) field, with a corresponding linear response susceptibility  $\chi_{LR}$ . In contrast, the (true) thermodynamic equilibrium susceptibility  $\chi_{eq}$  describes the situation, where the spin glass is allowed to relax to the thermodynamically most favored state in presence of a weak external field perturbation.

$$\chi_{LR} = \frac{1 - q_{EA}}{k_B T} \quad (44)$$

$$\chi_{eq} = \frac{\int dx (1 - \mathcal{Q}(x))}{k_B T} \quad (45)$$

Experimentally, the static linear-response susceptibility  $\chi_{LR}$  can be measured by looking at the response to a small external field perturbation  $h'$ , after cooling the system to the desired low temperature. In contrast, the equilibrium susceptibility  $\chi_{eq}$  is approximated by the field cooled susceptibility, which is measured by applying the small field perturbation already while cooling the system below the spin glass transition temperature. In this case, the sys-

tem has time to explore and select the most appropriate state while cooling in presence of the external perturbation. Experimental results of the two different spin glass susceptibilities below the critical temperature are illustrated for Cu(Mn13.5%) in Fig. 8 and compared with theoretical predictions.<sup>78,90</sup> In spin glass theory, e.g., the SK model, there is a clear distinction between replica symmetry breaking and hysteresis effects:<sup>78</sup> Hysteresis is commonly attributed to defects that are localized in space and induce a finite free energy barrier and thus finite lifetime of meta-stable states. Thus, in hysteresis, the two susceptibilities coincide after waiting sufficient long time. In contrast, the non-local barriers in spin glasses imply the re-arrangements in arbitrary large regions of the system, which can even diverge in the thermodynamic limit. Therefore, the different susceptibilities will not agree, provided that the externally applied field perturbation is sufficiently small.

Whether such a clear distinction between hysteresis and replica symmetry breaking also holds in a polaritonic setup is unknown and requires more experimental and theoretical work to demonstrate that polaritonic chemistry behaves as a spin glass system.<sup>91</sup> As we can deduce from the previous discussions, the quasi-static spin-glass picture of the SK model is incomplete for our polaritonic setup, since the dressed electronic structure of an ensemble of molecules under VSC will be (periodically) driven by the dynamics of the nuclear and displacement field coordinates. Therefore, it is likely that time-dependent external field perturbations are required to probe the coexistence of different cavity-induced linear (or higher-order) susceptibilities (see discussion in Sec. 4.2.2). In particular, we already see that Eq. (44) should explicitly depend on time, since the Edwards-Anderson order parameter of the cH equations directly depends on  $(R(t), q_\beta(t))$  and thus  $q_{EA}(t)$ . If this also implies the coexistence of different (possibly dynamic) susceptibilities under VSC remains a non-trivial open question. A further hint at interesting effects is the fact that we have now a highly degenerate ground state which makes response calculations intricate. However, investigating dynamic susceptibilities could provide a promising route to verify and characterize the proposed polarization-glass phase in a cavity.

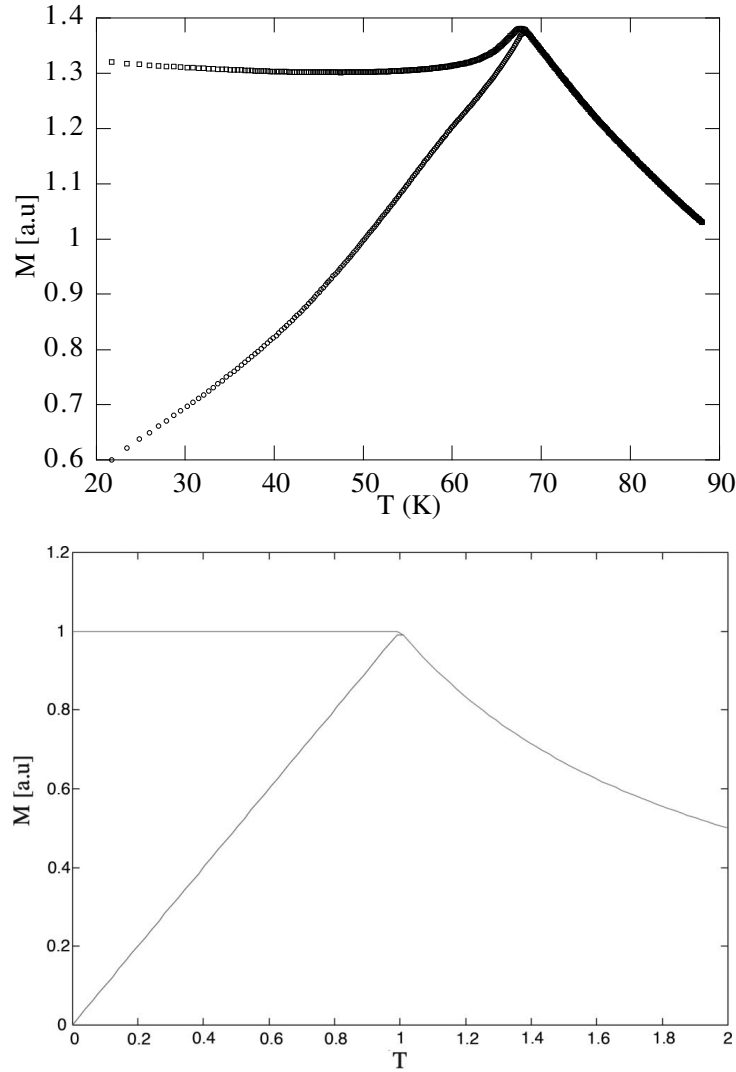


Figure 8: Comparison of experimental (top) and model (bottom) susceptibilities with respect to temperature  $T$ . The linear response susceptibility ( $\chi_{LR}$ , lower curve) can be measured experimentally by applying an external field perturbation after the cooling of the material (Cu(Mn13.5%)) below the critical spin glass temperature. In contrast, the equilibrium susceptibility ( $\chi_{eq}$ , upper curve) can be approximated experimentally by applying the magnetic field perturbation before the cooling.<sup>78,90</sup> Above the critical temperature the material enters the paramagnetic stable phase, with only one susceptibility, i.e., the linear response accesses equilibrium properties.

### 4.2.2 Off-equilibrium: Time-correlations and cavity-induced feedback effects

Even more interesting than the equilibrium properties of spin glasses are their associated off-equilibrium phenomena, which are observable for different materials. In order to measure the generalized susceptibility, it is common practice to rely on the fluctuation-dissipation theorem, which relates the response of the system to an external perturbation (weak off-equilibrium) to its equilibrium properties (fluctuations/correlations). The fluctuations of glassy systems can be characterized by the time-correlations of the magnetizations (or polarizations respectively),

$$C(t, t_w) = \frac{1}{N} \sum_i^N \langle \sigma_i(t_w) \sigma_i(t_w + t) \rangle \Rightarrow \frac{1}{N} \sum_i^N \frac{\langle \Delta\mu_i(t_w) \Delta\mu_i(t_w + t) \rangle}{\langle \Delta\mu_i(t_w) \Delta\mu_i(t_w) \rangle}. \quad (46)$$

Comparing the magnetization time-correlations of a (quasi-static) spin glass with the electronic correlations of a polarization glass reveals similarities (see Fig. 9) but again highlights some fundamental physical differences. In a spin glass, the magnetization correlations decay monotonically, but extremely slowly even on a logarithmic time-scale. In addition, the random process of  $\sigma_i(t)$  cannot be considered a wide-sense stationary stochastic process, which means the correlation does not only depend on the time-difference  $t$ , but also on the waiting-time  $t_w$  elapsed since entering the spin-glass phase. In other words, time-reversal symmetry is explicitly broken in a spin glass. The explicit waiting-time dependency will give rise to specific aging effects that are discussed in Sec. 4.2.3. In contrast, the polarization glass correlations reveal different oscillatory regimes, introduced by the time-dependent  $(R(t), q_\beta(t))$ -parameters. MD simulations with  $N = 36$  Shin-Metiu molecules reveal the following correlation features within an adiabatic regime:

1. Long-lived periodic (dynamic) correlation patterns emerge.
2. Fast oscillations (vibrational and cavity time scales) that are symmetrically distributed around  $C(t) = 0$  (light-blue), i.e., the existence of anti-correlated states.

3. The amplitude of the fast oscillations is modulated periodically on an order of magnitude smaller frequency scale (blue), with even coarser intensity modulations on a pico-second time scale.
4. The long-lived correlations are introduced by the harmonic nature of the strongly coupled cavity mode  $q_\beta$  and their overall magnitude depends on the losses of the cavity (a Langevin-thermostat is coupled to  $q_\beta$ , see Ref. 20 for implementation details). In particular, a more Brownian-like motion of  $q_\beta$  effectively prevents that long-lived correlations emerge. The Brownian dynamics of  $q_\beta$  can be interpreted as the weak coupling to a continuum of modes or thermal bath instead.

Investigating thoroughly the long-lived correlation dynamics in a polarization glass is already a computationally very demanding task. Particularly, the deviations of  $\Delta\mu_i(t)$  from a wide-sense stationary stochastic process are non-trivial to detect and thus remain an open research question. In particular, significant deviations may potentially only occur when increasing the collective coupling strength beyond the onset of the polarization glass instability. The breakdown of the adiabatic picture for the dressed electronic structure will increase the computational complexity even further in this regime, which may require the development of novel computational algorithms. However, the strongly oscillatory nature of the correlations within the adiabatic regime may also have immediate implications for the development of a dynamic susceptibility picture, as previously discussed. When averaging the (immediate) linear response susceptibilities over many oscillatory cycles, little to no effect (deviation from the mean) is expected. This suggests that higher-order response functions will likely become relevant observables to unravel the inner workings of a polarization glass and thus VSC in general. Overall, characterizing correlations, (non-linear) responses as well as non-adiabatic effects will have important implications for the off-equilibrium properties of a cavity-induced polarization glass. Particularly, non-adiabatic effects are known to essentially determine the physics of the SK model, as we detail in the following.

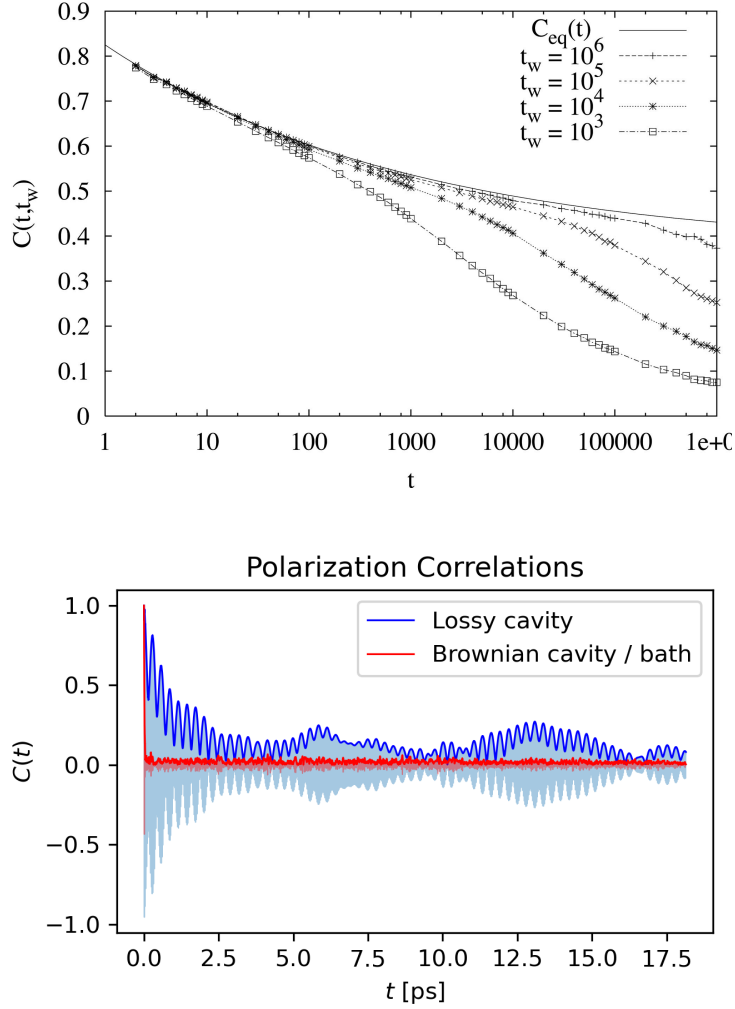


Figure 9: Comparison of time-correlations in a spin and polarization glass: **Top:** Monotonically decaying time correlation functions  $C(t, t_w)$  of an Ising spin glass (taken from Ref. 78 based on data from Ref. 92). The dependency on the waiting time  $t_w$  indicates the aging behaviour. **Bottom:** Oscillating polarization correlations of the Shin-Metiu setup under VSC with  $N = 36$  molecules. When calculating  $C(t)$  it was implicitly assumed that  $\Delta\mu_i(t)$  is a wide-sense stationary stochastic process within the adiabatic cH picture. The correlations oscillate fast (light-blue), on the time-scale of the cavity (vibrations), where the bold lines visualize the enveloping function. The blue line corresponds to the strong coupling to one lossy cavity mode ( $q_\beta$  weakly coupled to a Langevin bath). In contrast, the coupling to a Brownian mode is shown in red, which can be interpreted as the weak coupling to many cavity modes (thermal bath) instead.

### 4.2.3 Off-equilibrium: Breakdown of the fluctuation-dissipation theorem and aging effects

Let us next make the following assumptions: At time  $t_0 = 0$  the system is suddenly cooled below the critical glass temperature  $T < T_g$ , which triggers the phase transition into a spin glass. After a waiting time  $t_w$ , a constant external field perturbation  $h'$  is applied. Eventually, the response of the system  $S(t_w, t)$  is evaluated at time  $t + t_w \geq t_w$ . Under these conditions, the fluctuation-dissipation relations connect<sup>78,93,94</sup> the time correlation function of the total magnetization  $C(t, t_w)$ , defined in Eq. (46), to the average relaxation function per spin, which is defined by<sup>78</sup>

$$S(t, t_w) = k_B T \lim_{\delta h' \rightarrow 0} \frac{\delta \langle m(t_w + t) \rangle}{\delta h'}. \quad (47)$$

Eq. (47) describes the response of the magnetization at time  $t_w + t$  if the external field was added at time  $t_w$ . However, the standard fluctuation-dissipation theorem is only applicable if the system obeys the detailed balance condition,<sup>95</sup> which can be violated in a glassy system on longer time-scales. To account for this aspect, modified fluctuation dissipation relations have been proposed that hold for weak off-equilibrium.<sup>75,96,97</sup> In more detail, two different off-equilibrium regimes are distinguished for (spin) glasses, for which different fluctuation-dissipation relations hold:<sup>94</sup>

In the *stationary correlation regime* of a spin glass, the correlations are assumed to solely depend on  $t$ , but not on the waiting time  $t_w$ , i.e,  $C(t, t_w) = C_s(t)$ . Typically this approximation is reasonable only for relatively small  $t \approx 0$  in spin glasses, which implies high correlations  $C_s(t) \approx 1$ . Having correlations close to unity, the standard (thermal equilibrium) fluctuation-dissipation relation are applicable, which yields<sup>92,98</sup>

$$S(t) = 1 - C_s(t). \quad (48)$$

In the *aging regime*, where the correlations are no longer stationary, modified fluctuation-dissipation relations of the following form were suggested<sup>75</sup>

$$\frac{dS(t_w, t)}{dt} = X(C(t, t_w)) \frac{dC(t, t_w)}{dt}. \quad (49)$$

Again the SK model provides an ideal starting point to interpret Eq. (49) analytically, since one can show that  $C(t, t_w) = \frac{1}{N} \sum_i^N \langle \sigma_i(t_w) \rangle \langle \sigma_i(t_w + t) \rangle = q(t_w, t_w + t)$  in absence of an external magnetization field, i.e., for  $h_m = J_0 = 0$ .<sup>78</sup> This allows to discuss off-equilibrium effects in spin glasses analytically, in the absence of external magnetization fields. In more detail, by eliminating the time parametrically, one can re-express  $S(t_w, t) \mapsto S(t_w, C)$ . Afterwards, identifying  $X(C) = dS(t_w, C)/dC$  in the large waiting limit  $t_w \rightarrow \infty$ , one can relate the dynamic quantity  $X(C)$  to the equilibrium  $\mathfrak{x}(\mathfrak{q})$ , i.e.,  $X(C) = \mathfrak{s}(\mathfrak{q})|_{\mathfrak{q}=C}$ .<sup>75</sup> This leads to a simple physical picture in the aging regime in terms of the slope of the response with respect to the correlations, i.e.,<sup>78,93,96,99–101</sup>

$$\frac{dS}{dC} = X(C) = \int_0^C d\mathfrak{q} P(\mathfrak{q}). \quad (50)$$

In other words, the deviations of the fluctuation-dissipation theorem that are caused by aging effects can be related to equilibrium properties given by  $P(\mathfrak{q})$ . An illustration of the two different off-equilibrium regimes with their relation to equilibrium properties is given in Fig. 10a for the SK model in comparison with standard hysteresis effects, i.e., visualizing the difference between replica symmetry breaking and hysteresis. Notice the modifications of the fluctuation-dissipation relations can be re-interpreted in terms of an effective temperature<sup>97,100</sup>

$$\tau = -T \left( \frac{dS}{dC} \right)^{-1} \geq T \quad (51)$$

which indicates a heating or excess of thermal fluctuations since  $0 \leq dS/dC \leq 1$  according



to the probability interpretation of Eq. (50). The two different off-equilibrium regimes, i.e., the emergence of aging effects, seem to be a generic feature of glassy systems.<sup>75</sup> In Fig. 10b experimentally recorded fluctuation-dissipation relations are shown for  $\text{CdCr}_{1.7}\text{In}_{0.3}\text{S}_4$  with respect to different finite waiting times.<sup>102</sup> The extrapolation to infinite waiting times allows the connection to the theoretical spin glass models (i.e., the connecting to equilibrium properties).

Including the parametric feedback of the nuclei on the dressed electronic structure modifies the fluctuation-dissipation picture of a spin glass significantly. In particular, the emergence of periodic oscillations implies that the thermal equilibrium fluctuation-dissipation relation, given in Eq. (48), will no longer be applicable in the stationary correlation picture. This is not so surprising since the electronic subsystem is strongly correlated with the other subsystems (not decoupled, i.e. strongly hybridised). Therefore, Eq. (48) will remain valid solely for very short time-scales ( $C_s(t) \approx 1$ ), or if the cavity is too lossy/too weakly coupled to the system to induce any chemical changes on the molecular ensemble (see suppressed correlations visualized by the red line in Fig. 9). Consequently, different fluctuation-dissipation relations are expected even in the stationary correlation regime under VSC. Similarly, by increasing the collective coupling strength further, the breakdown of the adiabatic approximation suggest the emergence of a dynamic aging regime under VSC. In analogy to the stationary case, we expect that the dynamic feedback effects require modifications of the fluctuation-dissipation relation in Eq. (49) to be captured.

#### 4.2.4 Polaritonic resonance picture revised

As we know from a set of different experiments addressing a variety of chemical reactions in cavities (see e.g. Sec. 3.2), resonance effects play a major role when modifying chemical properties under collective VSC.<sup>22,103,104</sup> Thus it comes as no surprise that periodic feedback effects between the frustrated (off-equilibrium) electronic structure, the nuclear and cavity degrees of freedom and the thermal bath re-appear in a holistic theoretical descrip-

tion.<sup>5</sup> While considerable theoretical efforts went into investigating resonance effects with polaritonic reaction-rate theories<sup>67,105–110</sup> or few-molecule ab-initio simulations,<sup>111–113</sup> we believe that the polarization-glass concept provides a necessary link between the macroscopic (rates) and microscopic (few-molecule) chemical pictures. It opens up the door to identify prerequisites to observe chemical changes in a cavity from an ab-initio perspective. In more detail, we anticipate a scale-connecting resonance mechanism under collective VSC of a form similar to the following: Assuming that the losses of the cavity are sufficiently small (an effective cavity mode is distinguished), a dynamic instability (phase transition) of the dressed electronic structure can emerge for sufficiently strong collective couplings. The resulting polarization-glass phase introduces dynamic correlations between the electronic structures of the molecules. The long-lived correlations imply modifications of the standard (thermal) fluctuation-dissipation relations for the dressed electronic structure, which implies a different out-of-equilibrium description. Eventually, the dynamic (memory-dependent) electronic correlations will act back on the dynamics of the photon displacement field and the nuclei. In that regard, the dynamically frustrated nature of the electronic structure bridges not only length and time-scales, but it also breaks the conservative nature (in a system subspace) of the classical forces of Eq. (5). While the magnitude of the cavity-induced polarizations might be very small, their correlated and long-lived nature may still be sufficient to introduce stochastic resonance phenomena<sup>5</sup> at least for certain chemical systems and thus modifies their respective chemical properties. Clearly, the ab-initio picture of cavity-induced resonance effects remains vague at the moment and considerable theoretical and experimental effort will be required to unravel it and make it more quantitative and predictive. However, we believe that the spin-glass-like nature of the dressed electronic structure provides the most realistic and plausible theoretical framework that sets the necessary seed (instability mechanism) to trigger the resonance effects that have been observed in polaritonic experiments. Therefore, we consider the connection between polaritonic chemistry and the physics of a spin glass an excellent starting point to not only better understand current experimental findings, but

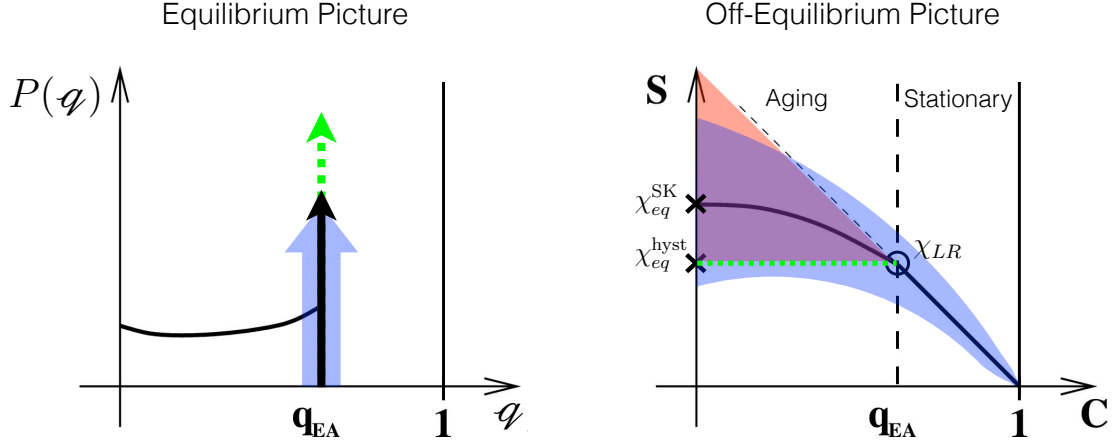
also to stimulate novel theoretical and experimental directions. This should allow us to reach a holistic understanding of strongly-coupled light and matter systems. Moreover, our connection provides an interesting new perspective to the applicability of the field of spin glasses beyond condensed matter systems.

## 5 Summary and Conclusion

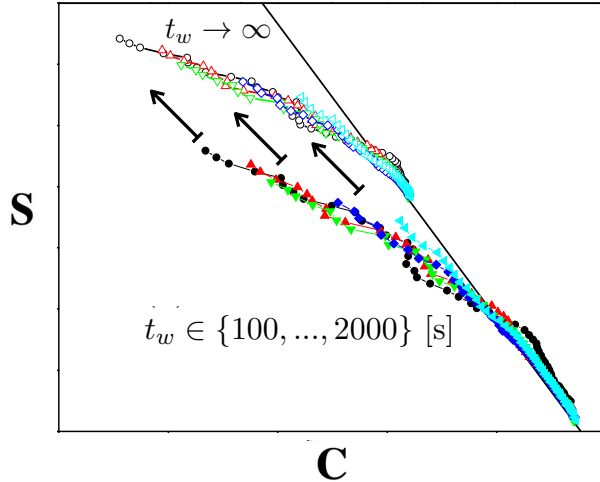
In this work we have established a novel connection between two separated and disconnected research areas: The emergent field of polaritonic chemistry and the long and widely studied complex field of spin glasses and rare events in statistical mechanics. The mapping of the static electronic structure problem of a dilute ensemble under collective VSC, onto the spin-glass model of Sherrington and Kirkpatrick suggests the emergence of a cavity-induced phase transition. The **static mapping** onto a spin glass indicates the following for the dressed electronic-structure problem:

1. Polarization ordering (polarization-glass phase transition) emerges for sufficiently strong collective light-matter couplings to the cavity modes.
2. Thermal and non-adiabatic effects can start to play a role for the collective electronic structure problem in a cavity, even though these effects can be usually disregarded for an ensemble in free-space.
3. Within the (static) polarization-glass phase, extremely long correlation times and frustration effects emerge, that do not only change equilibrium properties, but also give rise to off-equilibrium aging effects mediated by the long-range cavity modes, which can be re-interpreted as an effective heating of the system.

Overall the standard SK model of a spin glass suggests an instability of the dressed electronic subsystem altering the established temporal and spatial scales to understand chemistry on a molecular scale. Eventually, relaxing the restrictive static two-level approximation in



(a) Connecting equilibrium and off-equilibrium picture for a spin (black) and polarization (light blue) glass. **Left:** Equilibrium order parameter distribution of a SK model (black) taken from Ref. 114 in comparison with deviations of  $q_{EA}(t)$  in a cavity. **Right:** In spin glasses two different (weak) off-equilibrium regimes (stationary and aging) can be distinguished for a small external field perturbation  $h'$ , applied after a waiting time  $t_w$ . The stationary regime is governed by a linear fluctuation dissipation relation, which terminates at  $C = q_{EA}$  given by the linear response susceptibility  $S(q_{EA}) = T\chi_{LR}$ . In contrast, the aging regime is governed by the modified fluctuation dissipation relations in Eq. (49). It is bounded by the full thermal equilibrium susceptibility  $S(0) = T\chi_{eq}$  at  $C = 0$ . Notice that  $\chi_{eq} \neq \chi_{LR}$  indicates replica symmetry breaking, whereas  $\chi_{eq} = \chi_{LR}$  corresponds to normal hysteresis effects that do not require the complex theory of spin glasses to describe its equilibrium properties (dashed green). The slope of the curve can be interpreted as an effective temperature increase (see Eq. (51)) (red). The dynamic feedback effects in a cavity suggest the breakdown of the linear fluctuation-dissipation relations already within the stationary correlation regime (light-blue).



(b) Experimental off-equilibrium measurement: The breakdown of fluctuation-dissipation relations (aging) measured the after cooling  $\text{CdCr}_{1.7}\text{In}_{0.3}\text{S}_4$  below the critical spin glass temperature of  $T_g = 16.2$  K. Bold symbols indicate the measured relaxation-correlation curve for different (finite) waiting times  $t_w \in \{100, 200, 500, 1000, 2000\}$  [s]. Open symbols show the extrapolation to infinite waiting times  $t_w \rightarrow \infty$ . The illustration was modified based on Fig. 7 Ref. 75, which contains experimental data from Ref. 102.

the SK mapping breaks with the established picture of spin glasses. The non-perturbative feedback effect between the dressed electronic problem and the oscillating nuclei and cavity field introduces dynamically frustrated correlations, which require novel concepts and theoretical methods. For instance, the non-monotonic behavior of the correlations in the dynamical situation (see Fig. 9) modifies the simple heating-picture for off-equilibrium effects and could allow cooling as well. Such effects have recently been observed experimentally for collective strong-coupling situations.<sup>115</sup> The numerical results suggest the following **dynamical features of a polarization glass** at the onset of the instability (adiabatic electronic ground-state approximation):

1. For a fixed time-step, the polarizations are anti-aligned and narrowly distributed, which gives rise to significant dynamical frustration/correlation effects with zero overall polarization (absence of chemical shifts in NMR experiments<sup>27</sup>).
2. The dynamical feedback between cavity, nuclei and electronic structure introduces a configuration-dependent (time-dependent) Edwards-Anderson order parameter.
3. The cavity-induced polarizations oscillate and are correlated over very long time-scales, which modifies the thermal fluctuation-dissipation relations. However, in the adiabatic limit no waiting time dependency has been detected with our present simulation capabilities and thus aging effects have not (yet) been verified under VSC.

Simulations **beyond the adiabatic approximation** would be required to fully enter the polarization glass phase, which will become computationally extremely demanding (solving the time-dependent Schrödinger equation and including temperature). However, from the SK model, one can anticipate that spontaneous replica symmetry breaking may also start to play a role. Therefore, one would expect the emergence of dynamical aging effects and thus a cavity-induced **time-reversal symmetry breaking**. This complicates the theoretical picture even further, particularly if reaching for an analytic understanding in the large- $N$  limit. However, cavity-induced time-reversal symmetry breaking could also open novel pathways

for the sub-field of chiral polaritonics.<sup>116</sup> There the common aim is to reach cavity-induced enantioselectivity by explicitly parity-violating cavity polarizations.<sup>112,117–123</sup> However, from a fundamental theoretical aspect similar effects may also be reached by spontaneous symmetry breaking instead.<sup>124,125</sup> Eventually, from a theoretical chemistry perspective, the even more pressing theoretical question is how the feedback between the electronic, nuclear and cavity subsystems can give rise to the experimentally observed **stochastic resonance phenomena**, as suggested in Sec. 4.2.4. We expect that the instability and thus the dynamical frustration of the dressed electronic structure acts as a seed such that stochastic resonances emerge, i.e., a synchronization of the nuclear/cavity dynamics builds up. However, this picture remains to be proved/disproved. Yet if validated (or supplemented) it could be used as a guiding principle for the design of experimental VSC setups and for the development of effective models of polaritonic chemistry.

## Acknowledgement

We gratefully acknowledge all members of our ERC synergy grant proposal team (Tal Schwartz, Thomas Ebbesen, Abraham Nitzan, Sharly Fleischer, Cyriaque Genet and Maxim Sukharev) for inspiring discussions and helpful comments. This work was made possible through the support of the RouTe Project (13N14839), financed by the Federal Ministry of Education and Research (Bundesministerium für Bildung und Forschung (BMBF)) and supported by the European Research Council (ERC-2015-AdG694097), the Cluster of Excellence “CUI: Advanced Imaging of Matter” of the Deutsche Forschungsgemeinschaft (DFG), EXC 2056, project ID 390715994 and the Grupos Consolidados (IT1249-19). The Flatiron Institute is a division of the Simons Foundation.).

## Supporting Information Available

### References

- (1) Zewail, A. H. Laser Femtochemistry. *Science* **1988**, *242*, 1645–1653.
- (2) Zewail, A. H. Femtochemistry. Past, present, and future. *Pure and Applied Chemistry* **2000**, *72*, 2219–2231.
- (3) Ebbesen, T. W. Hybrid Light–Matter States in a Molecular and Material Science Perspective. *Accounts of Chemical Research* **2016**, *49*, 2403–2412.
- (4) Ruggenthaler, M.; Tancogne-Dejean, N.; Flick, J.; Appel, H.; Rubio, A. From a quantum-electrodynamical light–matter description to novel spectroscopies. *Nature Reviews Chemistry* **2018**, *2*, 0118.
- (5) Sidler, D.; Ruggenthaler, M.; Schäfer, C.; Ronca, E.; Rubio, A. A perspective on ab initio modeling of polaritonic chemistry: The role of non-equilibrium effects and quantum collectivity. *The Journal of Chemical Physics* **2022**, *156*, 230901.
- (6) Fregoni, J.; Garcia-Vidal, F. J.; Feist, J. Theoretical Challenges in Polaritonic Chemistry. *ACS Photonics* **2022**, *9*, 1096–1107.
- (7) Ebbesen, T. W.; Rubio, A.; Scholes, G. D. Introduction: Polaritonic Chemistry. *Chemical Reviews* **2023**, *123*, 12037–12038.
- (8) Ruggenthaler, M.; Sidler, D.; Rubio, A. Understanding Polaritonic Chemistry from Ab Initio Quantum Electrodynamics. *Chemical Reviews* **2023**, *123*, 11191–11229.
- (9) Bhuyan, R.; Mony, J.; Kotov, O.; Castellanos, G. W.; Gómez Rivas, J.; Shegai, T. O.; Börjesson, K. The Rise and Current Status of Polaritonic Photochemistry and Photophysics. *Chemical Reviews* **2023**, *123*, 10877–10919.

- (10) Hirai, K.; Hutchison, J. A.; Uji-i, H. Molecular Chemistry in Cavity Strong Coupling. *Chemical Reviews* **2023**, *123*, 8099–8126.
- (11) Simpkins, B. S.; Dunkelberger, A. D.; Vurgaftman, I. Control, Modulation, and Analytical Descriptions of Vibrational Strong Coupling. *Chemical Reviews* **2023**, *123*, 5020–5048.
- (12) Mandal, A.; Taylor, M. A.; Weight, B. M.; Koessler, E. R.; Li, X.; Huo, P. Theoretical Advances in Polariton Chemistry and Molecular Cavity Quantum Electrodynamics. *Chemical Reviews* **2023**, *123*, 9786–9879.
- (13) Xiang, B.; Xiong, W. Molecular Polaritons for Chemistry, Photonics and Quantum Technologies. *Chemical Reviews* **2024**, *124*, 2512–2552.
- (14) Garcia-Vidal, F. J.; Ciuti, C.; Ebbesen, T. W. Manipulating matter by strong coupling to vacuum fields. *Science* **2021**, *373*, eabd0336.
- (15) Flick, J.; Ruggenthaler, M.; Appel, H.; Rubio, A. Atoms and molecules in cavities, from weak to strong coupling in quantum-electrodynamics (QED) chemistry. *Proceedings of the National Academy of Sciences* **2017**, *114*, 3026–3034.
- (16) Svendsen, M. K.; Ruggenthaler, M.; Hübener, H.; Schäfer, C.; Eckstein, M.; Rubio, A.; Latini, S. Theory of Quantum Light-Matter Interaction in Cavities: Extended Systems and the Long Wavelength Approximation. 2023; <https://arxiv.org/abs/2312.17374>, Version Number: 1.
- (17) Sidler, D.; Schäfer, C.; Ruggenthaler, M.; Rubio, A. Polaritonic Chemistry: Collective Strong Coupling Implies Strong Local Modification of Chemical Properties. *The Journal of Physical Chemistry Letters* **2021**, *12*, 508–516.
- (18) Schnappinger, T.; Sidler, D.; Ruggenthaler, M.; Rubio, A.; Kowalewski, M. Cavity Born–Oppenheimer Hartree–Fock Ansatz: Light–Matter Properties of Strongly



- Coupled Molecular Ensembles. *The Journal of Physical Chemistry Letters* **2023**, *14*, 8024–8033.
- (19) Sidler, D.; Ruggenthaler, M.; Rubio, A. Numerically Exact Solution for a Real Polaritonic System under Vibrational Strong Coupling in Thermodynamic Equilibrium: Loss of Light–Matter Entanglement and Enhanced Fluctuations. *Journal of Chemical Theory and Computation* **2023**, *19*, 8801–8814.
- (20) Sidler, D.; Schnappinger, T.; Obzhairov, A.; Ruggenthaler, M.; Kowalewski, M.; Rubio, A. Unraveling a Cavity-Induced Molecular Polarization Mechanism from Collective Vibrational Strong Coupling. *The Journal of Physical Chemistry Letters* **2024**, *15*, 5208–5214.
- (21) Hutchison, J. A.; Schwartz, T.; Genet, C.; Devaux, E.; Ebbesen, T. W. Modifying Chemical Landscapes by Coupling to Vacuum Fields. *Angewandte Chemie International Edition* **2012**, *51*, 1592–1596.
- (22) Thomas, A.; George, J.; Shalabney, A.; Dryzhakov, M.; Varma, S. J.; Moran, J.; Chervy, T.; Zhong, X.; Devaux, E.; Genet, C.; Hutchison, J. A.; Ebbesen, T. W. Ground-State Chemical Reactivity under Vibrational Coupling to the Vacuum Electromagnetic Field. *Angewandte Chemie* **2016**, *128*, 11634–11638.
- (23) Lather, J.; Bhatt, P.; Thomas, A.; Ebbesen, T. W.; George, J. Cavity Catalysis by Cooperative Vibrational Strong Coupling of Reactant and Solvent Molecules. *Angewandte Chemie International Edition* **2019**, *58*, 10635–10638.
- (24) Hirai, K.; Takeda, R.; Hutchison, J. A.; Uji-i, H. Modulation of Prins Cyclization by Vibrational Strong Coupling. *Angewandte Chemie* **2020**, *132*, 5370–5373.
- (25) Fukushima, T.; Yoshimitsu, S.; Murakoshi, K. Inherent Promotion of Ionic Conductivity via Collective Vibrational Strong Coupling of Water with the Vacuum Electromagnetic Field. *Journal of the American Chemical Society* **2022**, *144*, 12177–12183.

- (26) Ahn, W.; Triana, J. F.; Recabal, F.; Herrera, F.; Simpkins, B. S. Modification of ground-state chemical reactivity via light–matter coherence in infrared cavities. *Science* **2023**, *380*, 1165–1168.
- (27) Patrahau, B.; Piejko, M.; Mayer, R. J.; Antheaume, C.; Sangchai, T.; Ragazzon, G.; Jayachandran, A.; Devaux, E.; Genet, C.; Moran, J.; Ebbesen, T. W. Direct Observation of Polaritonic Chemistry by Nuclear Magnetic Resonance Spectroscopy. *Angewandte Chemie International Edition* **2024**, e202401368.
- (28) Fidler, A. P.; Chen, L.; McKillop, A. M.; Weichman, M. L. Ultrafast dynamics of CN radical reactions with chloroform solvent under vibrational strong coupling. *The Journal of Chemical Physics* **2023**, *159*, 164302.
- (29) Chen, L.; Fidler, A. P.; McKillop, A. M.; Weichman, M. L. Exploring the impact of vibrational cavity coupling strength on ultrafast CN + *c*-C<sub>6</sub>H<sub>12</sub> reaction dynamics. *Nanophotonics* **2024**, *13*, 2591–2599.
- (30) Mezard, M.; Parisi, G.; Virasoro, M. A. *Spin glass theory and beyond*; World Scientific lecture notes in physics v. 9; World Scientific: Singapore ; New Jersey, 1987; OCLC: ocm14929802.
- (31) Spohn, H. *Dynamics of Charged Particles and their Radiation Field*, 1st ed.; Cambridge University Press, 2023.
- (32) Hugall, J. T.; Singh, A.; Van Hulst, N. F. Plasmonic Cavity Coupling. *ACS Photonics* **2018**, *5*, 43–53.
- (33) Vahala, K. J. Optical microcavities. *Nature* **2003**, *424*, 839–846.
- (34) Törmä, P.; Barnes, W. L. Strong coupling between surface plasmon polaritons and emitters: a review. *Reports on Progress in Physics* **2015**, *78*, 013901.

- (35) Chang, D.; Douglas, J.; González-Tudela, A.; Hung, C.-L.; Kimble, H. *Colloquium* : Quantum matter built from nanoscopic lattices of atoms and photons. *Reviews of Modern Physics* **2018**, *90*, 031002.
- (36) Skolnick, M. S.; Fisher, T. A.; Whittaker, D. M. Strong coupling phenomena in quantum microcavity structures. *Semiconductor Science and Technology* **1998**, *13*, 645–669.
- (37) Flick, J.; Welakuh, D. M.; Ruggenthaler, M.; Appel, H.; Rubio, A. Light–Matter Response in Nonrelativistic Quantum Electrodynamics. *ACS Photonics* **2019**, *6*, 2757–2778.
- (38) Svendsen, M. K.; Thygesen, K. S.; Rubio, A.; Flick, J. *Ab Initio* Calculations of Quantum Light–Matter Interactions in General Electromagnetic Environments. *Journal of Chemical Theory and Computation* **2024**, *20*, 926–936.
- (39) Rokaj, V.; Welakuh, D. M.; Ruggenthaler, M.; Rubio, A. Light–matter interaction in the long-wavelength limit: no ground-state without dipole self-energy. *Journal of Physics B: Atomic, Molecular and Optical Physics* **2018**, *51*, 034005.
- (40) Schäfer, C.; Ruggenthaler, M.; Rokaj, V.; Rubio, A. Relevance of the Quadratic Diamagnetic and Self-Polarization Terms in Cavity Quantum Electrodynamics. *ACS Photonics* **2020**, *7*, 975–990.
- (41) Flick, J.; Appel, H.; Ruggenthaler, M.; Rubio, A. Cavity Born–Oppenheimer Approximation for Correlated Electron–Nuclear–Photon Systems. *Journal of Chemical Theory and Computation* **2017**, *13*, 1616–1625.
- (42) Schäfer, C.; Ruggenthaler, M.; Rubio, A. *Ab initio* nonrelativistic quantum electrodynamics: Bridging quantum chemistry and quantum optics from weak to strong coupling. *Physical Review A* **2018**, *98*, 043801.

- (43) Hoffmann, N. M.; Schäfer, C.; Rubio, A.; Kelly, A.; Appel, H. Capturing vacuum fluctuations and photon correlations in cavity quantum electrodynamics with multi-trajectory Ehrenfest dynamics. *Physical Review A* **2019**, *99*, 063819.
- (44) Chen, H.-T.; Li, T. E.; Sukharev, M.; Nitzan, A.; Subotnik, J. E. Ehrenfest+R dynamics. I. A mixed quantum–classical electrodynamics simulation of spontaneous emission. *The Journal of Chemical Physics* **2019**, *150*, 044102.
- (45) Li, T. E.; Nitzan, A.; Sukharev, M.; Martinez, T.; Chen, H.-T.; Subotnik, J. E. Mixed quantum-classical electrodynamics: Understanding spontaneous decay and zero-point energy. *Physical Review A* **2018**, *97*, 032105.
- (46) Chen, H.-T.; Li, T. E.; Sukharev, M.; Nitzan, A.; Subotnik, J. E. Ehrenfest+R dynamics. II. A semiclassical QED framework for Raman scattering. *The Journal of Chemical Physics* **2019**, *150*, 044103.
- (47) Hoffmann, N. M.; Schäfer, C.; Säkkinen, N.; Rubio, A.; Appel, H.; Kelly, A. Benchmarking semiclassical and perturbative methods for real-time simulations of cavity-bound emission and interference. *The Journal of Chemical Physics* **2019**, *151*, 244113.
- (48) Fregoni, J.; Corni, S.; Persico, M.; Granucci, G. Photochemistry in the strong coupling regime: A trajectory surface hopping scheme. *Journal of Computational Chemistry* **2020**, *41*, 2033–2044.
- (49) Li, T. E.; Nitzan, A.; Subotnik, J. E. Collective Vibrational Strong Coupling Effects on Molecular Vibrational Relaxation and Energy Transfer: Numerical Insights via Cavity Molecular Dynamics Simulations\*\*. *Angewandte Chemie* **2021**, *133*, 15661–15668.
- (50) Tavis, M.; Cummings, F. W. Exact Solution for an N -Molecule—Radiation-Field Hamiltonian. *Physical Review* **1968**, *170*, 379–384.

- (51) Galego, J.; Garcia-Vidal, F. J.; Feist, J. Cavity-Induced Modifications of Molecular Structure in the Strong-Coupling Regime. *Physical Review X* **2015**, *5*, 041022.
- (52) Schäfer, C. Polaritonic Chemistry from First Principles via Embedding Radiation Reaction. *The Journal of Physical Chemistry Letters* **2022**, *13*, 6905–6911.
- (53) Haugland, T. S.; Ronca, E.; Kjønstad, E. F.; Rubio, A.; Koch, H. Coupled Cluster Theory for Molecular Polaritons: Changing Ground and Excited States. *Physical Review X* **2020**, *10*, 041043.
- (54) Mordovina, U.; Bungey, C.; Appel, H.; Knowles, P. J.; Rubio, A.; Manby, F. R. Polaritonic coupled-cluster theory. *Physical Review Research* **2020**, *2*, 023262.
- (55) Rivera, N.; Flick, J.; Narang, P. Variational Theory of Nonrelativistic Quantum Electrodynamics. *Physical Review Letters* **2019**, *122*, 193603.
- (56) Ahrens, A.; Huang, C.; Beutel, M.; Covington, C.; Varga, K. Stochastic Variational Approach to Small Atoms and Molecules Coupled to Quantum Field Modes in Cavity QED. *Physical Review Letters* **2021**, *127*, 273601.
- (57) Schäfer, C.; Buchholz, F.; Penz, M.; Ruggenthaler, M.; Rubio, A. Making ab initio QED functional(s): Nonperturbative and photon-free effective frameworks for strong light–matter coupling. *Proceedings of the National Academy of Sciences* **2021**, *118*, e2110464118.
- (58) Sidler, D.; Ruggenthaler, M.; Appel, H.; Rubio, A. Chemistry in Quantum Cavities: Exact Results, the Impact of Thermal Velocities, and Modified Dissociation. *The Journal of Physical Chemistry Letters* **2020**, *11*, 7525–7530.
- (59) Yang, J.; Ou, Q.; Pei, Z.; Wang, H.; Weng, B.; Shuai, Z.; Mullen, K.; Shao, Y. Quantum-electrodynamical time-dependent density functional theory within Gaussian atomic basis. *The Journal of Chemical Physics* **2021**, *155*, 064107.

- (60) Welakuh, D. M.; Flick, J.; Ruggenthaler, M.; Appel, H.; Rubio, A. Frequency-Dependent Sternheimer Linear-Response Formalism for Strongly Coupled Light–Matter Systems. *Journal of Chemical Theory and Computation* **2022**, *18*, 4354–4365.
- (61) Kadanoff, L. P. More is the Same; Phase Transitions and Mean Field Theories. *Journal of Statistical Physics* **2009**, *137*, 777–797.
- (62) Golse, F.; Mouhot, C.; Paul, T. On the Mean Field and Classical Limits of Quantum Mechanics. *Communications in Mathematical Physics* **2016**, *343*, 165–205.
- (63) Lu, I.-T.; Ruggenthaler, M.; Tancogne-Dejean, N.; Latini, S.; Penz, M.; Rubio, A. Electron-photon exchange-correlation approximation for quantum-electrodynamical density-functional theory. *Physical Review A* **2024**, *109*, 052823.
- (64) Hutter, J. Car–Parrinello molecular dynamics. *WIREs Computational Molecular Science* **2012**, *2*, 604–612.
- (65) Schuch, N.; Verstraete, F. Computational complexity of interacting electrons and fundamental limitations of density functional theory. *Nature Physics* **2009**, *5*, 732–735.
- (66) Shin, S.; Metiu, H. Nonadiabatic effects on the charge transfer rate constant: A numerical study of a simple model system. *The Journal of Chemical Physics* **1995**, *102*, 9285–9295.
- (67) Li, X.; Mandal, A.; Huo, P. Cavity frequency-dependent theory for vibrational polariton chemistry. *Nature Communications* **2021**, *12*, 1315.
- (68) Hu, D.; Mandal, A.; Weight, B. M.; Huo, P. Quasi-diabatic propagation scheme for simulating polariton chemistry. *The Journal of Chemical Physics* **2022**, *157*, 194109.
- (69) Fischer, E. W.; Saalfrank, P. Beyond Cavity Born–Oppenheimer: On Nonadiabatic

- Coupling and Effective Ground State Hamiltonians in Vibro-Polaritonic Chemistry. *Journal of Chemical Theory and Computation* **2023**, *19*, 7215–7229.
- (70) Zhu, X.; Gu, B. Making Peace with Random Phases: Ab Initio Conical Intersection Quantum Dynamics in Random Gauges. *The Journal of Physical Chemistry Letters* **2024**, *15*, 8487–8493.
- (71) Fiechter, M. R.; Richardson, J. O. Understanding the cavity Born–Oppenheimer approximation. *The Journal of Chemical Physics* **2024**, *160*, 184107.
- (72) Horak, J.; Sidler, D.; Huang, W.-M.; Ruggenthaler, M.; Rubio, A. Analytic Model for Molecules Under Collective Vibrational Strong Coupling in Optical Cavities. 2024; <http://arxiv.org/abs/2401.16374>, arXiv:2401.16374 [physics, physics:quant-ph].
- (73) Edwards, S. F.; Anderson, P. W. Theory of spin glasses. *Journal of Physics F: Metal Physics* **1975**, *5*, 965–974.
- (74) Sherrington, D.; Kirkpatrick, S. Solvable Model of a Spin-Glass. *Physical Review Letters* **1975**, *35*, 1792–1796.
- (75) Parisi, G. Nobel Lecture: Multiple equilibria. *Reviews of Modern Physics* **2023**, *95*, 030501.
- (76) Alcón, I.; Ribas-Ariño, J.; Moreira, I. D. P.; Bromley, S. T. Emergent Spin Frustration in Neutral Mixed-Valence 2D Conjugated Polymers: A Potential Quantum Materials Platform. *Journal of the American Chemical Society* **2023**, *145*, 5674–5683.
- (77) Almeida, J. R. L. D.; Thouless, D. J. Stability of the Sherrington-Kirkpatrick solution of a spin glass model. *Journal of Physics A: Mathematical and General* **1978**, *11*, 983–990.
- (78) Parisi, G. Spin glasses and fragile glasses: Statics, dynamics, and complexity. *Proceedings of the National Academy of Sciences* **2006**, *103*, 7948–7955.

- (79) Thouless, D. J.; Anderson, P. W.; Palmer, R. G. Solution of 'Solvable model of a spin glass'. *Philosophical Magazine* **1977**, *35*, 593–601.
- (80) Parisi, G. Infinite Number of Order Parameters for Spin-Glasses. *Physical Review Letters* **1979**, *43*, 1754–1756.
- (81) Atkins, P. W.; Friedman, R. *Molecular quantum mechanics*, 5th ed.; Oxford Univ. Press: Oxford, 2011.
- (82) Schachenmayer, J.; Genes, C.; Tignone, E.; Pupillo, G. Cavity-Enhanced Transport of Excitons. *Physical Review Letters* **2015**, *114*, 196403.
- (83) Hagenmüller, D.; Schachenmayer, J.; Schütz, S.; Genes, C.; Pupillo, G. Cavity-Enhanced Transport of Charge. *Physical Review Letters* **2017**, *119*, 223601.
- (84) Bethe, H. A. Statistical theory of superlattices. *Proceedings of the Royal Society of London. Series A - Mathematical and Physical Sciences* **1935**, *150*, 552–575.
- (85) Parisi, G. A sequence of approximated solutions to the S-K model for spin glasses. *Journal of Physics A: Mathematical and General* **1980**, *13*, L115–L121.
- (86) Guerra, F. Broken Replica Symmetry Bounds in the Mean Field Spin Glass Model. *Communications in Mathematical Physics* **2003**, *233*, 1–12.
- (87) Talagrand, M. The parisi formula. *Annals of Mathematics* **2006**, *163*, 221–263.
- (88) Alvarez Baños, R. et al. Nature of the spin-glass phase at experimental length scales. *Journal of Statistical Mechanics: Theory and Experiment* **2010**, *2010*, P06026.
- (89) Alvarez Baños, R. et al. Static versus Dynamic Heterogeneities in the  $D = 3$  Edwards-Anderson-Ising Spin Glass. *Physical Review Letters* **2010**, *105*, 177202.
- (90) Djurberg, C.; Jonason, K.; Nordblad, P. Magnetic relaxation phenomena in a CuMn spin glass. *The European Physical Journal B* **1999**, *10*, 15–21.



- (91) Schwartz, T.; Ebbesen, T. W.; Rubio, A.; Nitzan, A. ERC Synergy Grant Research Proposal 2024: Unraveling the Mysteries of Vibrational Strong Coupling. 2024.
- (92) Marinari, E.; Parisi, G.; Ricci-Tersenghi, F.; Ruiz-Lorenzo, J. J. Violation of the fluctuation-dissipation theorem in finite-dimensional spin glasses. *Journal of Physics A: Mathematical and General* **1998**, *31*, 2611–2620.
- (93) Cugliandolo, L. F.; Kurchan, J. On the out-of-equilibrium relaxation of the Sherrington-Kirkpatrick model. *Journal of Physics A: Mathematical and General* **1994**, *27*, 5749–5772.
- (94) Franz, S.; Virasoro, M. A. Quasi-equilibrium interpretation of ageing dynamics. *Journal of Physics A: Mathematical and General* **2000**, *33*, 891–905.
- (95) Kubo, R.; Toda, M.; Hashitsume, N. In *Statistical Physics II*; Cardona, M., Fulde, P., Von Klitzing, K., Queisser, H.-J., Lotsch, H. K. V., Eds.; Springer Series in Solid-State Sciences; Springer Berlin Heidelberg: Berlin, Heidelberg, 1991; Vol. 31.
- (96) Cugliandolo, L. F.; Kurchan, J. Analytical solution of the off-equilibrium dynamics of a long-range spin-glass model. *Physical Review Letters* **1993**, *71*, 173–176.
- (97) Franz, S.; Mézard, M.; Parisi, G.; Peliti, L. Measuring Equilibrium Properties in Aging Systems. *Physical Review Letters* **1998**, *81*, 1758–1761.
- (98) Baity-Jesi, M. et al. A statics-dynamics equivalence through the fluctuation-dissipation ratio provides a window into the spin-glass phase from nonequilibrium measurements. *Proceedings of the National Academy of Sciences* **2017**, *114*, 1838–1843.
- (99) Franz, S.; Mézard, M. Off-Equilibrium Glassy Dynamics: A Simple Case. *Europhysics Letters (EPL)* **1994**, *26*, 209–214.

- (100) Cugliandolo, L. F.; Kurchan, J.; Peliti, L. Energy flow, partial equilibration, and effective temperatures in systems with slow dynamics. *Physical Review E* **1997**, *55*, 3898–3914.
- (101) Franz, S.; Mézard, M.; Parisi, G.; Peliti, L. The Response of Glassy Systems to Random Perturbations: A Bridge Between Equilibrium and Off-Equilibrium. *Journal of Statistical Physics* **1999**, *97*, 459–488.
- (102) Hérisson, D.; Ocio, M. Fluctuation-Dissipation Ratio of a Spin Glass in the Aging Regime. *Physical Review Letters* **2002**, *88*, 257202.
- (103) Thomas, A.; Lethuillier-Karl, L.; Nagarajan, K.; Vergauwe, R. M. A.; George, J.; Chervy, T.; Shalabney, A.; Devaux, E.; Genet, C.; Moran, J.; Ebbesen, T. W. Tilting a ground-state reactivity landscape by vibrational strong coupling. *Science* **2019**, *363*, 615–619.
- (104) Thomas, A.; Jayachandran, A.; Lethuillier-Karl, L.; Vergauwe, R. M.; Nagarajan, K.; Devaux, E.; Genet, C.; Moran, J.; Ebbesen, T. W. Ground state chemistry under vibrational strong coupling: dependence of thermodynamic parameters on the Rabi splitting energy. *Nanophotonics* **2020**, *9*, 249–255.
- (105) Li, X.; Mandal, A.; Huo, P. Theory of Mode-Selective Chemistry through Polaritonic Vibrational Strong Coupling. *The Journal of Physical Chemistry Letters* **2021**, *12*, 6974–6982.
- (106) Yang, P.-Y.; Cao, J. Quantum Effects in Chemical Reactions under Polaritonic Vibrational Strong Coupling. *The Journal of Physical Chemistry Letters* **2021**, *12*, 9531–9538.
- (107) Mandal, A.; Li, X.; Huo, P. Theory of vibrational polariton chemistry in the collective coupling regime. *The Journal of Chemical Physics* **2022**, *156*, 014101.

- (108) Lindoy, L. P.; Mandal, A.; Reichman, D. R. Resonant Cavity Modification of Ground-State Chemical Kinetics. *The Journal of Physical Chemistry Letters* **2022**, *13*, 6580–6586.
- (109) Cao, J. Generalized Resonance Energy Transfer Theory: Applications to Vibrational Energy Flow in Optical Cavities. *The Journal of Physical Chemistry Letters* **2022**, *13*, 10943–10951.
- (110) Ke, Y.; Richardson, J. O. Quantum nature of reactivity modification in vibrational polariton chemistry. *The Journal of Chemical Physics* **2024**, *161*, 054104.
- (111) Schäfer, C.; Flick, J.; Ronca, E.; Narang, P.; Rubio, A. Shining light on the microscopic resonant mechanism responsible for cavity-mediated chemical reactivity. *Nature Communications* **2022**, *13*, 7817.
- (112) Sun, S.; Gu, B.; Mukamel, S. Polariton ring currents and circular dichroism of Mg-porphyrin in a chiral cavity. *Chemical Science* **2022**, *13*, 1037–1048.
- (113) Philbin, J. P.; Wang, Y.; Narang, P.; Dou, W. Chemical Reactions in Imperfect Cavities: Enhancement, Suppression, and Resonance. *The Journal of Physical Chemistry C* **2022**, *126*, 14908–14913.
- (114) Parisi, G.; Ricci-Tersenghi, F.; Ruiz-Lorenzo, J. J. Generalized off-equilibrium fluctuation-dissipation relations in random Ising systems. *The European Physical Journal B* **1999**, *11*, 317–325.
- (115) Jarc, G.; Mathengattil, S. Y.; Montanaro, A.; Giusti, F.; Rigoni, E. M.; Sergio, R.; Fassioli, F.; Winnerl, S.; Dal Zilio, S.; Mihailovic, D.; Prelovšek, P.; Eckstein, M.; Fausti, D. Cavity-mediated thermal control of metal-to-insulator transition in 1T-TaS<sub>2</sub>. *Nature* **2023**, *622*, 487–492.

- (116) Bustamante, C. M.; Sidler, D.; Ruggenthaler, M.; Rubio, A. The relevance of degenerate states in chiral polaritonics. 2024; <https://arxiv.org/abs/2408.16695>, Version Number: 1.
- (117) Hübener, H.; De Giovannini, U.; Schäfer, C.; Andberger, J.; Ruggenthaler, M.; Faist, J.; Rubio, A. Engineering quantum materials with chiral optical cavities. *Nature Materials* **2021**, *20*, 438–442.
- (118) Schlawin, F.; Kennes, D. M.; Sentef, M. A. Cavity quantum materials. *Applied Physics Reviews* **2022**, *9*, 011312.
- (119) Voronin, K.; Taradin, A. S.; Gorkunov, M. V.; Baranov, D. G. Single-Handedness Chiral Optical Cavities. *ACS Photonics* **2022**, *9*, 2652–2659.
- (120) Mauro, L.; Fregoni, J.; Feist, J.; Avriller, R. Chiral discrimination in helicity-preserving Fabry-Pérot cavities. *Physical Review A* **2023**, *107*, L021501.
- (121) Baranov, D. G.; Schäfer, C.; Gorkunov, M. V. Toward Molecular Chiral Polaritons. *ACS Photonics* **2023**, *10*, 2440–2455.
- (122) Riso, R. R.; Grazioli, L.; Ronca, E.; Giovannini, T.; Koch, H. Strong Coupling in Chiral Cavities: Nonperturbative Framework for Enantiomer Discrimination. *Physical Review X* **2023**, *13*, 031002.
- (123) Riso, R. R.; Ronca, E.; Koch, H. Strong Coupling to Circularly Polarized Photons: Toward Cavity-Induced Enantioselectivity. *The Journal of Physical Chemistry Letters* **2024**, *15*, 8838–8844.
- (124) Greiner, W.; Reinhardt, J. *Field Quantization*; Springer Berlin Heidelberg: Berlin, Heidelberg, 1996.
- (125) Srednicki, M. *Quantum Field Theory*; Cambridge University Press: Cambridge, 2007.